Disorder-free localization in continuous-time quantum walks: Role of symmetries

A. P. Balachandran,[1,*] Anjali Kundalpady,[2,†] Pramod Padmanabhan,[3,‡] and Akash Sinha[3,§]
[1]*Department of Physics, Syracuse University, Syracuse, New York 13244-1130, USA*
[2]*International Centre for Theoretical Sciences, Survey No. 151, Shivakote, Hesaraghatta Hobli, Bengaluru 560089, India*
[3]*School of Basic Sciences, Indian Institute of Technology, Bhubaneswar 752050, India*

(Received 13 July 2023; revised 22 October 2023; accepted 15 December 2023; published 9 January 2024)

We investigate the phenomenon of disorder-free localization in quantum systems with global permutation symmetry. We use permutation group theory to systematically construct permutation-symmetric many-fermion Hamiltonians and interpret them as generators of continuous-time quantum walks. When the number of fermions is very large we find that all the canonical basis states localize at all times, without the introduction of any disorder coefficients. This time-independent localization is not the result of any emergent disorder, distinguishing it from existing mechanisms for disorder-free localization. Next we establish the conditions under which the localization is preserved. We find that interactions that preserve and break the global permutation symmetry sustain localization. Furthermore, the basis states of systems with reduced permutation symmetry localize even for a small number of fermions when the symmetry-reducing parameters are tuned accordingly. We show that similar localization also occurs for a permutation-symmetric Heisenberg spin chain and permutation-symmetric bosonic systems, implying that the localization is independent of the superselected symmetry. Finally, we make connections of the Hamiltonians studied here to the adjacency matrices of graphs and use this to propose a prescription for disorder-free localization in continuous-time quantum walk systems. Many of the models proposed here feature all-to-all connectivity and can be potentially realized on superconducting quantum circuits, trapped ion systems, and ultracold atoms.

DOI: 10.1103/PhysRevA.109.012205

I. INTRODUCTION

A closed many-body system is described by a few parameters (temperature, pressure, etc.) once it attains equilibrium. This thermal behavior, while true in nonintegrable classical systems, may not always hold for their quantum analogs where the effects of destructive interference among the constituents can result in localized states that are nonthermal [1,2], thus violating the eigenstate thermalization hypothesis [3–6]. The typical mechanism to produce such states is to use random potentials or introduce disorder coefficients in the Hamiltonian. However, there exist methods to produce localized states without disorder, now known as disorder-free localization (DFL), showing that disorder is just a sufficient feature and not necessary. Systems showing this phenomenon include lattice gauge theories [7–10] and the so-called Stark many-body localization (MBL) models [11–14], among others [15–18]. In many of these systems the disorder is emergent in the Hilbert space dynamics, resulting in the ergodicity-breaking property.

In this work we show a completely different origin of DFL in systems with and without superselected and global symmetries. Our method is to use the properties of the spectrum of Hamiltonians to produce localization of states in Hilbert space. We observe that systems where one eigenvalue has a large degeneracy compared to others can result in Hilbert space localization without any disorder. We construct such Hamiltonians in Fock space and find that all the basis states of each number sector localize. Before we proceed further, we will clarify the definition of localization we will use. Consider a state $|\psi\rangle$, a basis element of some number sector of the Fock space, evolving under a Hamiltonian H. If the probability distribution computed from the overlap between $|\psi(t)\rangle = e^{-iHt}|\psi(0)\rangle$ and $|\psi(0)\rangle$ stays close to one at all times, we say that the state $|\psi\rangle$ is localized.[1,2] In other words, the time-evolved states in this system retain memory of the initial states at all times t. This definition implies that the states of our systems localize in Hilbert space. Due to this, there is no notion of localization lengths for our states and in this regard it is similar to localization via MBL states [21].

The systems we consider include various symmetries including superselected symmetries. Typically, a quantum theory with superselection sectors is tightly constrained, restricting the possible representations that the algebra of observables can take. The operators of such theories commute with the superselected symmetries and the Hilbert space splits

*apbal1938@gmail.com
†anjali.kundalpady@gmail.com
‡pramod23phys@gmail.com
§akash.sinha@gmail.com

[1]This quantity is also related to the Loschmidt echo [19,20].
[2]In this definition, eigenstates of the system will be localized. For the systems we study we will consider localized states that does not include the eigenstates.

into different superselection sectors that are labeled by the irreducible representations of the superselected symmetries. A physically important example of such a symmetry is the permutation symmetry generated by the statistics operator that occurs while studying a system of identical and indistinguishable bosons (fermions). In such theories the states are symmetrized (antisymmetrized) and the operators are invariant under this exchange symmetry.

In general, such systems, though constrained, are not expected to show nonthermal behavior. For example, the tight-binding Hamiltonian of fermions or bosons does not show any localization without disorder. In this work we will exhibit several fermionic Hamiltonians with and without global symmetries that show DFL. To construct these models we begin with a many-fermion Hamiltonian with global permutation symmetry $\mathcal{S}_N$. This Hamiltonian is number preserving and we find that all the canonical basis states in each fermion number sector localizes without any disorder for large N. The requirement of the global $\mathcal{S}_N$ symmetry enforces the interaction of each fermion with every other fermion, making the Hamiltonian similar in appearance to the Sachdev-Ye-Kitaev (SYK) model [22–25]. Our naive intuition might suggest that such a system where all particles interact with each other should thermalize. On the contrary, we see complete localization in their dynamics. It is also worth noting that there is no emergent disorder in the models described here, unlike the gauged models in the literature that exhibit DFL. Our construction also considers permutation-symmetric operators in higher-fermion number sectors, which can be thought of as interactions. The localization is stable to the inclusion of such terms. Additionally, there are terms that break the global $\mathcal{S}_N$ symmetry but preserve the localization. We show several examples of such terms which both preserve and destroy the localization.

Furthermore, the models we write down can be interpreted as quantum walk Hamiltonians that have received a great deal of attention in the past [26–31] in the context of search algorithms [32–34], as quantum simulators [35–38], and for universal quantum computation [39–42]. We are concerned with continuous-time quantum walks of identical particles [43–49] and especially those with an additional global symmetry. Symmetric quantum walks have been considered in the case of discrete-time quantum walks [50–52] and have been shown to feature topological phases [53–56] and localization [57–61].

The rest of the article is organized as follows. We begin Sec. II with the space describing the fermions and the operators acting on them. The Hamiltonians with global $\mathcal{S}_N$ symmetry are constructed using simple ideas from the theory of permutation groups. Among the many possibilities, we consider the simplest such Hamiltonian in Sec. II. The solution of the Hamiltonian is provided in Sec. III and the resulting features are compared with the models that lack a global $\mathcal{S}_N$ symmetry.

In a rather long discussion in Sec. IV, we explore several other models that both display and break the DFL discussed for the $\mathcal{S}_N$-symmetric model in the first part of the paper. In particular, we study the effect of perturbations that break the global symmetry in Sec. IV A. Next we study when the localization persists for different initial conditions in Sec. IV B. In Sec. IV C we analyze the role played by the global symmetry in the localization and find that a fermionic model with a reduced global symmetry ($\mathcal{S}_N \to \mathcal{S}_{N-k}$) can also exhibit localization. We note here that a spin system with a global $\mathcal{S}_N$ symmetry and a permutation-symmetric bosonic system also display similar localization features. Then we highlight an interesting connection of these systems to adjacency matrices of graphs in Sec. IV D. This connection suggests a possible way to generalize the DFL studied in this work. We then conclude in Sec. V with a few remarks about experimental realizations and future theoretical directions.

II. CONSTRUCTION

We begin with a brief description of the Fock space (spanned by the states diagonalizing the number operator) describing N identical and indistinguishable fermions. The vacuum $|\Omega\rangle$ denotes the state with no fermions. The state $|i\rangle$, for $i \in \{1, 2, \ldots, N\}$, describes the presence of a fermion on site i. These are the one-fermion states and they span an N-dimensional space, henceforth denoted $\mathcal{H} \simeq \mathbb{C}^N$ with the canonical inner product. In this notation, multiparticle states such as $|i\rangle \otimes |j\rangle$ exist in $\mathcal{H} \otimes \mathcal{H}$. No relation between $|i\rangle \otimes |j\rangle$ and $|j\rangle \otimes |i\rangle$ is assumed *a priori*. However, in the case of indistinguishable fermions, we work with normalized antisymmetrized states $\frac{1}{\sqrt{2}}[|i\rangle \otimes |j\rangle - |j\rangle \otimes |i\rangle]$ that exist in $\mathcal{H} \wedge \mathcal{H}$, with the $\wedge$ denoting antisymmetrization. Thus the full Hilbert space becomes the antisymmetrized Fock space $\bigoplus_{n=0}^{N} \mathcal{H}^{\wedge n}$. This space is finite and its dimension is seen from

$$\sum_{k=0}^{N} \binom{N}{k} = 2^N,$$

with $\binom{N}{k}$ the dimension of $\underbrace{\mathcal{H} \wedge \mathcal{H} \wedge \cdots \wedge \mathcal{H}}_{k \text{ times}}$.

The creation ($a_j^\dagger$) and annihilation (a_j) operators satisfying the fermionic [self-dual canonical anticommutation relation (CAR)] algebra

$$\begin{aligned} \{a_j, a_k^\dagger\} &= \delta_{jk}, \\ \{a_j, a_k\} &= \{a_j^\dagger, a_k^\dagger\} = 0, \end{aligned} \tag{2.1}$$

where $\{a, b\} := ab + ba$, are realized in this space. The index j take values in $\{1, \ldots, N\}$. More generally, we could add an extra index μ to each oscillator to denote an internal degree of freedom like a color or spin index. For simplicity, we will stick to just the indices $j \in \{1, 2, \ldots, N\}$ for the fermions, allowing their interpretation as lattice sites.

An arbitrary k-fermion state expressed as

$$a_{i_1}^\dagger a_{i_2}^\dagger \cdots a_{i_k}^\dagger |\Omega\rangle \tag{2.2}$$

satisfies all the necessary antisymmetry properties, as can be directly verified by using (2.1). With the help of these a and $a^\dagger$, we can mutate between different particle sectors. For example, the action of $a_i^\dagger$ on an arbitrary state from $\mathcal{H}^{\wedge k}$ yields

$$a_i^\dagger (a_{i_1}^\dagger a_{i_2}^\dagger \cdots a_{i_k}^\dagger |\Omega\rangle) = a_i^\dagger a_{i_1}^\dagger a_{i_2}^\dagger \cdots a_{i_k}^\dagger |\Omega\rangle \in \mathcal{H}^{\wedge k+1}. \tag{2.3}$$

The Fock space description ensures that the fermionic creation and annihilation operators commute with the superselected exchange symmetry of this system.

Next we move on to the action of the global permutation symmetry $\mathcal{S}_N$ on the site indices $\{1, 2, \ldots, N\}$. The action of these operators on the states and operators of the theory are obtained as follows. The vacuum is invariant under permutations $s_{ij}|\Omega\rangle = |\Omega\rangle$ and the transformation rule of operators under conjugation by permutation generators is $s_{jk} O_{\ldots j \ldots k \ldots} s_{jk}^{-1} = O_{\ldots k \ldots j \ldots}$, where O is an operator with several indices including j and k (note that $s_{jk}^{-1} = s_{jk}$). Using these properties, we can deduce the action of the permutation group on arbitrary states of this system.

Permutation-invariant operators acting on these states satisfy

$$s_i O_{i_1 \cdots i_p} s_i = O_{i_1 \cdots i_p} \; \forall\, i \in \{1, 2, \ldots, N-1\}, \tag{2.4}$$

where $s_i \equiv s_{i,i+1}$ are the transposition operators that generate the permutation group ($\mathcal{S}_N$) and satisfy

$$s_i s_{i+1} s_i = s_{i+1} s_i s_{i+1}, \;\; s_i^2 = 1, \;\; s_i s_j = s_j s_i \text{ for } |i-j| \geqslant 2. \tag{2.5}$$

For the particular value of $N = 2$, let us consider the two operators

$$a_1^\dagger a_1 + a_2^\dagger a_2, \quad a_1^\dagger a_2 + a_2^\dagger a_1. \tag{2.6}$$

They clearly are invariant under the action of $\mathcal{S}_2$ and the objective is to construct such permutation-invariant operators for arbitrary $\mathcal{S}_N$. A natural place to look for such objects is in the conjugacy classes of $\mathcal{S}_N$ which are left invariant as a set under the action of the group by definition. For the permutation group, the elements of a conjugacy class have the same cycle structure and their order is given by

$$\frac{N!}{\prod_{k=1}^{N} (k^{\nu_k}) \nu_k!},$$

where ν_k is the number of k-cycles. A clear invariance is the sum of the elements of a given conjugacy class with a particular cycle structure.[3] These statements are independent of the particular realization of the transposition operators. For our current problem we will show a realization using the fermionic creation and annihilation operators. The operators we use are such that the resulting Hamiltonians are Hermitian and number preserving as the permutation operators do not change the number of fermions.

We will obtain the fermionic realization of $\mathcal{S}_N$ by showing the existence of the permutation operators for each particle sector. The fermionic realization for a generic transposition permutation $\sigma \in \mathcal{S}_N$ in the k-fermion sector is given by

$$\sigma = \sum_{i_1 < i_2 < \cdots < i_k} a_{\sigma(i_1)}^\dagger a_{\sigma(i_2)}^\dagger \cdots a_{\sigma(i_k)}^\dagger a_{i_k} \cdots a_{i_2} a_{i_1}. \tag{2.7}$$

The permutation σ has a particular cycle structure. For example, the fermionic realizations of the transpositions (ij) in the one-fermion and two-fermion sectors are given by

$$(ij)_1 = a_j^\dagger a_i + a_i^\dagger a_j + \sum_{\substack{k=1 \\ k \neq i,j}}^{N} a_k^\dagger a_k \tag{2.8}$$

and

$$(ij)_2 = a_j^\dagger a_i^\dagger a_j a_i + \sum_{k \neq j} a_j^\dagger a_k^\dagger a_k a_i + \sum_{k \neq i} a_k^\dagger a_i^\dagger a_j a_k + \sum_{\substack{k,l=1^N \\ k<l \neq \{i,j\}}} a_k^\dagger a_l^\dagger a_l a_k, \tag{2.9}$$

respectively. The subscript α on $(ij)_\alpha$ denotes the fermion number sector on which this transposition acts. Thus, in the full Fock space the transposition is given by

$$(ij) = \bigoplus_{\alpha=1}^{N} (ij)_\alpha. \tag{2.10}$$

A more nontrivial example is that of a three-cycle permutation in the one-fermion sector

$$(ijk)_1 = a_j^\dagger a_i + a_k^\dagger a_j + a_i^\dagger a_k + \sum_{\substack{l=1 \\ l \neq \{i,j,k\}}}^{N} a_l^\dagger a_l. \tag{2.11}$$

Note that the Hermitian conjugate of this term is $(ikj)_1$. Indeed, the Hamiltonian identified as a sum of the elements of the conjugacy class will turn out to be Hermitian. We can now write an $\mathcal{S}_N$-invariant Hamiltonian for a given conjugacy class made of p-cycles as

$$H^{(p)} = \bigoplus_{\alpha=1}^{N} H_\alpha^{(p)}, \tag{2.12}$$

where

$$H_\alpha^{(p)} = \sum_{i_1 < i_2 < \cdots < i_p} (i_1 i_2 \cdots i_p)_\alpha \tag{2.13}$$

acts on the α-fermion sector. Such $\mathcal{S}_N$-invariant Hamiltonians (2.12) are true for any realization of the permutation group. The fermionic realization in (2.7) introduces simplifications to the Hamiltonian due to the CAR algebra (2.1).

Before going into these, we first note that the operators corresponding to cycles of length larger than β annihilate the vectors in the β-fermionic sector. Thus the bilinear expression acting on the one-fermion sector affects all possible fermion number sectors in a system of N fermions. It acts as an exchange operator on the one-fermion states and has a nontrivial action on the remaining sectors.

In what follows we will restrict ourselves to the Hamiltonians constructed out of the two-cycle conjugacy class. We will comment on models obtained from other conjugacy classes in Sec. IV; however, a more detailed investigation is beyond the scope of the present work.

Two-cycle Hamiltonian

Consider the conjugacy class made out of purely 2-cycles which are just the transpositions. They include the exchange of any two of the N indices and there are precisely $\frac{N(N-1)}{2}$ of them. The two-cycle Hamiltonian in the one-fermion sector is obtained using (2.8) and is bilinear in the fermion creation and

[3]These are precisely the generators of the center of the permutation group algebra $\mathbb{C}(\mathcal{S}_N)$.

annihilation operators,

$$H_1^{(2)} = \sum_{i<j}[a_i^\dagger a_j + a_j^\dagger a_i] + \frac{(N-1)(N-2)}{2}\hat{N}. \tag{2.14}$$

The factor accompanying the number operator $\hat{N} = \sum_{k=1}^N a_k^\dagger a_k$ is a result of the substitution (2.8) for the 2-cycles. Clearly, the term in square brackets commutes with $\hat{N}$ and represents a fermion on a given site hopping to any other site. As noted earlier, this Hamiltonian has a nontrivial action on every fermion number sector except on the one-fermion sector where it acts as a permutation operator. It is clearly $\mathcal{S}_N$ invariant in its site indices.[4] The second term in (2.14) dominates for large N. Our goal is to study the localization features of this system for large N and so the explicit presence of N in the Hamiltonian can lead to incorrect conclusions about the origin of the localization. To avoid this we will choose the term in square brackets as our Hamiltonian

$$H = \sum_{i<j}[a_i^\dagger a_j + a_j^\dagger a_i], \tag{2.15}$$

where all the fermions interact with each other in a symmetrical manner. This model can be solved exactly by a simple change of basis, as we will see in Sec. III.

In addition to the above bilinear Hamiltonian, we consider the operators acting on the two-fermion states which are quartic in the fermion creation and annihilation operators. This Hamiltonian can be thought of as an interaction term when added to the bilinear Hamiltonian in (2.15). However, a crucial point is that this two-cycle Hamiltonian can be simplified[5] using the CAR algebra in (2.1), resulting in

$$H_2^{(2)} = \left(\frac{(N-2)(N-3)}{2} - 1\right)(\hat{N}^2 - \hat{N}) + 2\sum_{i<j}[a_i^\dagger a_j + a_j^\dagger a_i](\hat{N} - 1). \tag{2.16}$$

This Hamiltonian continues to remain $\mathcal{S}_N$ invariant and acts on two-fermion and higher-fermion states. These terms represent interactions but reduce to the product of bilinear operators due to the CAR algebra. As a consequence, they commute with the Hamiltonian in (2.14) and thus merely shift their eigenvalues while sharing the eigenstates. This further implies that localized states of (2.15) are stable to such $\mathcal{S}_N$-preserving perturbations. This trend continues to hold for higher-order perturbations obtained using the two-cycle Hamiltonians acting on three- and higher-fermion sectors (see Appendix B).

III. SOLUTION

The bilinear Hamiltonian in (2.15) is solved with a simple change of variables in the space of creation and annihilation operators. Consider a new set of annihilation and creation) operators A_α and $A_\alpha^\dagger$ defined as

$$A_\alpha = \frac{1}{\sqrt{N}}\sum_{j=1}^N \omega^{j\alpha} a_j, \quad A_\alpha^\dagger = \frac{1}{\sqrt{N}}\sum_{j=1}^N \omega^{-j\alpha} a_j^\dagger, \tag{3.1}$$

with $\omega = e^{2\pi \mathrm{i}/N}$ the Nth root of unity and $\alpha \in \{1, 2, \ldots, N\}$. These operators satisfy the CAR relations required of fermionic operators

$$\{A_\alpha, A_\beta^\dagger\} = \delta_{\alpha\beta},$$
$$\{A_\alpha, A_\beta\} = \{A_\alpha^\dagger, A_\beta^\dagger\} = 0. \tag{3.2}$$

In these variables, the two-cycle Hamiltonian in (2.15) reduces to

$$H = NA_N^\dagger A_N - \hat{N}, \tag{3.3}$$

where $\hat{N} = \sum_{i=1}^N a_i^\dagger a_i = \sum_{\alpha=1}^N A_\alpha^\dagger A_\alpha$ commutes with the Hamiltonian. A number of fermionic symmetries for the Hamiltonian in (3.3) become apparent in this basis. We find that all bilinear operators[6] $A_\alpha^\dagger A_\beta$, $A_\alpha A_\beta$, and $A_\alpha^\dagger A_\beta^\dagger$ commute with the Hamiltonian when $\alpha, \beta \neq N$. In fact, the permutation operators of (2.7) can be written as linear combinations of such bilinear operators and thus these are the operators that map the states of a given eigenspace onto each other.

The spectrum can be found by labeling the eigenspaces with the set $\{1, 2, \ldots, N\}$. The dimension of the k-fermion sector is $\frac{N!}{k!(N-k)!}$ and this is spanned by two kinds of eigenstates of the form

$$A_{\alpha_1}^\dagger A_{\alpha_2}^\dagger \cdots A_{\alpha_k}^\dagger |\Omega\rangle, \tag{3.4}$$

where no two α's are equal to each other. The first set of eigenstates are those where at least one of the α's is N. There is a total of $\frac{(N-1)!}{(k-1)!(N-k)!}$ such states and they share the eigenvalue $N-k$. The second set consists of those eigenstates where none of the α's take the value N. These account for the remaining $\frac{(N-1)!}{k!(N-k-1)!}$ states and they come with the eigenvalue $-k$. In evaluating the spectrum we use the identities

$$[\hat{N}, A_\alpha^\dagger] = A_\alpha^\dagger, \quad [\hat{N}, A_\alpha] = -A_\alpha. \tag{3.5}$$

Having obtained the spectrum, we are in a position to compute the probability distributions. We consider one-fermion and two-fermion walks, which sufficiently illustrate the features of the permutation-invariant systems considered here. Following this, we also discuss the general k-fermion sector. An important point to keep in mind is the role played by the global $\mathcal{S}_N$ symmetry in determining the structure of the spectrum. For instance, it is enough to find the time evolution of any single state in a particular number sector. The remaining states can be computed by the action of the appropriate $\mathcal{S}_N$ operators on this state. Furthermore, another crucial feature arises as a consequence of the global $\mathcal{S}_N$ symmetry, namely,

[4] A more rigorous proof is shown in Appendix A.

[5] The proof for this is shown in Appendix B.

[6] Removing the number operator from (3.3) will enhance the number of fermionic symmetries as now A_α and $A_\alpha^\dagger$ will also commute with the Hamiltonian when $\alpha \neq N$.

the restriction on the subspace that a given state is allowed to evolve into. For example, the two-fermion state $|1, 2(t)\rangle := \exp(-iHt)a_1^\dagger a_2^\dagger|\Omega\rangle$ only evolves into the $|1, j\rangle$ and $|2, j\rangle$ states. There is no overlap with the states $|j, k\rangle := a_j^\dagger a_k^\dagger|\Omega\rangle$ when $j, k \notin \{1, 2\}$. In other words, any state in this system does not explore the full Hilbert space under time evolution. This is not apparent from the A_α or $A_\alpha^\dagger$ basis but becomes more transparent in a new basis. We will demonstrate this for each of the fermion number sectors below.

A. One-fermion walks

The features we wish to illustrate are immediately seen in the following eigenbasis of the one-fermion sector: There is one state of the form

$$\sum_{j=1}^{N} a_j^\dagger|\Omega\rangle, \tag{3.6}$$

with eigenvalue $N-1$, and there are $N-1$ eigenstates of the form

$$(a_1^\dagger - a_j^\dagger)|\Omega\rangle, \quad j \in \{2, 3, \ldots, N\}, \tag{3.7}$$

with eigenvalue -1. The nondegenerate state in (3.6) is symmetric under the action of $\mathcal{S}_N$, whereas the degenerate states in (3.7) are mapped onto each other under the action of $\mathcal{S}_N$. More precisely, the transposition operators in the one-fermion sector (2.8) perform this mapping. These operators can be written as linear combinations of the bilinear operators $A_\alpha^\dagger A_\beta$ and as noted earlier these commute with the Hamiltonian (3.3).

The nonzero probability distributions are found to be

$$|\langle 1|1(t)\rangle|^2 = \frac{1}{N^2}[1 + (N-1)^2 + 2(N-1)\cos(Nt)], \tag{3.8}$$

$$|\langle j|1(t)\rangle|^2 = \frac{2}{N^2}[1 - \cos(Nt)] \tag{3.9}$$

for $j \in \{2, 3, \ldots, N\}$ and $|j(t)\rangle = e^{-iHt}|j\rangle$ are the time-evolved states. The nonoscillating terms of both these expressions highlight the localization effect. For large N the term in (3.8) goes to 1 whereas the term in (3.9) goes to 0. These features are illustrated in Fig. 1(e). The reason for the restricted evolution can also be seen from the explicit structure of the unitary evolution operator in the one-fermion sector and this is shown in Appendix E.

The phase of the oscillating term in (3.8) and (3.9) is the difference between the two energy levels in the one-fermion sector. We have seen earlier that the addition of higher-order interaction terms (2.10) will only shift these energy levels of the Hamiltonian (2.15), leaving the structure of the eigenstates intact. This implies that the localization seen here is stable to the inclusion of such $\mathcal{S}_N$-symmetric interactions. This argument continues to hold even in the k-fermion sector as there are just two energy levels in each fermion number sector.

B. Two-fermion walks

Using the eigenstates in (3.4), the amplitude for an initial two-fermion state $|i, j\rangle$ to end up in a state $|k, l\rangle$ after a time t is found to be

$$\langle k, l|i, j(t)\rangle = \frac{1}{N^2}\Bigg(e^{-i(N-2)t}\sum_{\alpha=1}^{N-1}(\omega^{i\alpha} - \omega^{j\alpha})(\omega^{-k\alpha} - \omega^{-l\alpha}) + e^{2it}\sum_{\substack{\alpha,\beta=1\\ \alpha<\beta}}^{N-1}(\omega^{i\alpha+j\beta} - \omega^{i\beta+j\alpha})(\omega^{-k\alpha-l\beta} - \omega^{-l\alpha-k\beta})\Bigg), \tag{3.10}$$

where $|i, j(t)\rangle$ are the time-evolved two-fermion states. As mentioned earlier, the restricted evolution is not apparent from (3.10), but it becomes more transparent in a changed basis for the two-fermion states.[7] Consider the normalized eigenstates

$$|[j]\rangle_2 = \frac{1}{\sqrt{N-1}}a_j^\dagger\sum_{\substack{i=1\\ i\neq j}}^{N} a_i^\dagger|\Omega\rangle, \quad j \in \{1, 2, \ldots, N-1\}, \tag{3.11}$$

$$|[jkN]\rangle_2 = \frac{1}{\sqrt{3}}(a_j^\dagger a_k^\dagger + a_k^\dagger a_N^\dagger + a_N^\dagger a_j^\dagger)|\Omega\rangle, \quad j < k \in \{1, 2, \ldots, N-1\}. \tag{3.12}$$

For these two sets of states, the notation $|[\,]\rangle_2$ indicates that it is a linear combination of two-fermion states. From these expressions we see that there are $N-1$ eigenstates of this form in (3.11) and they come with the eigenvalue $N-2$ and there are $\frac{(N-1)(N-2)}{2}$ states of the form (3.12) with eigenvalue -2. This is consistent with the previous solution. As in the one-fermion sector, the $\mathcal{S}_N$ symmetries, generated using (2.9), map the degenerate eigenstates onto each other. These operators can be written as products of the bilinear operators in $A_\alpha^\dagger A_\beta$ and hence commute with the Hamiltonian in (3.3).

These eigenstates are used to expand $|1, 2\rangle = a_1^\dagger a_2^\dagger|\Omega\rangle$ as

$$|1, 2\rangle = \frac{\sqrt{N-1}}{N}(|[1]\rangle_2 - |[2]\rangle_2) + \frac{\sqrt{3}(N-2)}{N}|[12N]\rangle_2 - \frac{\sqrt{3}}{N}\sum_{j=3}^{N-1}(|[1jN]\rangle_2 - |[2jN]\rangle_2). \tag{3.13}$$

The first three states in the above expression, $|[1]\rangle_2$, $|[2]\rangle_2$, and $|[12N]\rangle_2$, are linear combinations of $|1, j\rangle$ and $|2, j\rangle$ with $j \in \{1, \ldots, N\}$. The states under the summation, $|[1jN]\rangle_2$ and $|[2jN]\rangle_2$, also contain the $|j, N\rangle$ states, but these cancel while taking the difference of these two states. Thus, from these arguments it is clear that the time-evolved $|1, 2\rangle$ state will not overlap with a state $|j, k\rangle$ where neither j nor k is (1,2). This is verified in the plot for the probability distribution shown in Fig. 1(c). This is to be contrasted with a similar plot for a Hamiltonian that is not permutation invariant [see Fig. 1(d)], where the two fermions can now be found in states that do not

[7]The orthogonality and completeness of these states are discussed in Appendix C.

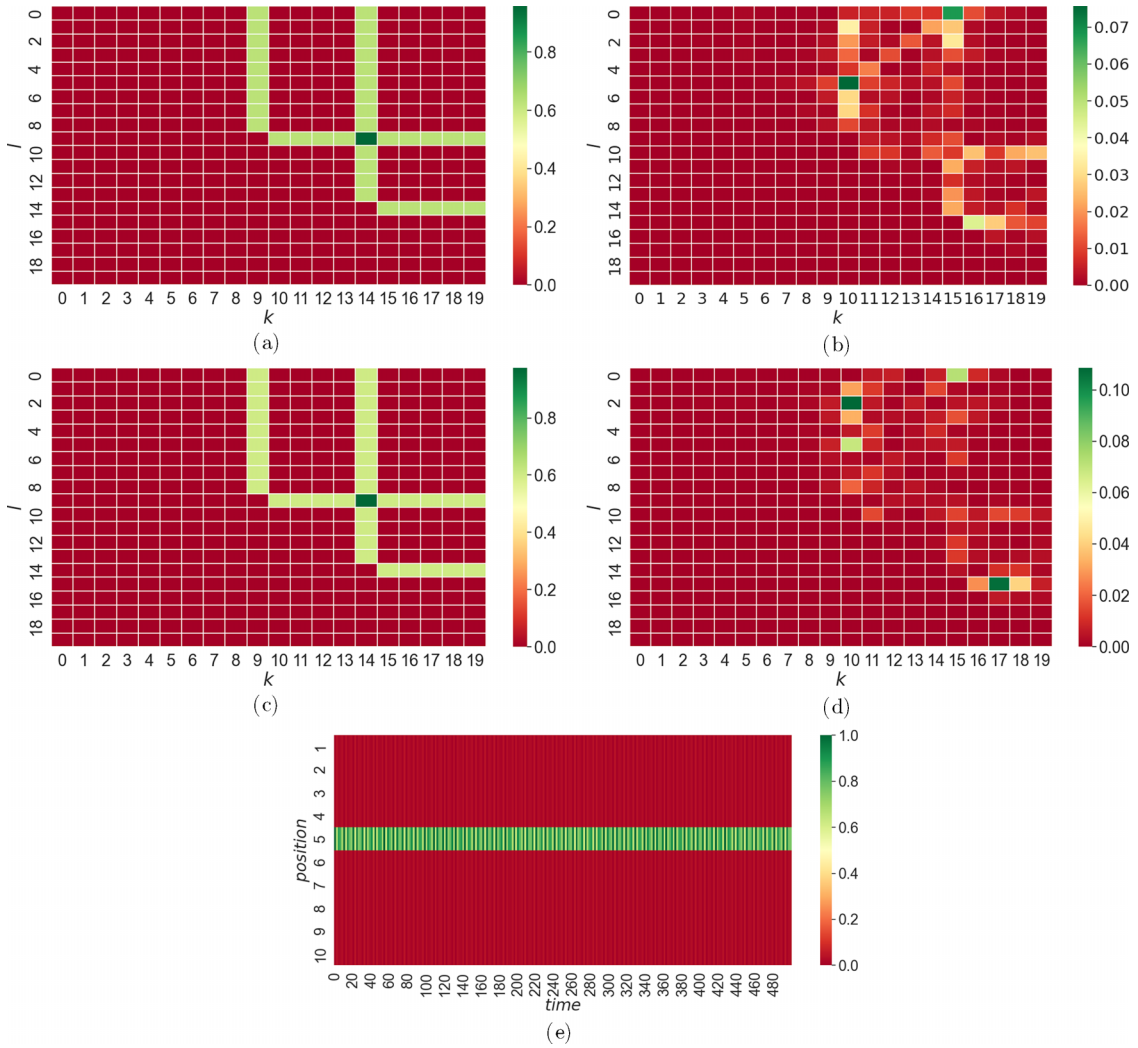

FIG. 1. Probability distributions for the symmetric Hamiltonian (2.15) and the tight-binding Hamiltonian $\sum_{j=1}^{N} a_j^\dagger a_{j+1} + \text{H.c.}$ Localization is observed for the former. (a) Two-fermion walk in the symmetric case, with the probability for the initial position ($l = 9, k = 14$) at $t = 3$. (b) Two-fermion walk in the tight-binding case, with the probability for the initial position ($l = 9, k = 14$) at $t = 3$. (c) Two-fermion walk in the symmetric case, with the probability for the initial position ($l = 9, k = 14$) at $t = 3000$. (d) Two-fermion walk in the tight-binding case, with the probability for the initial position ($l = 9, k = 14$) at $t = 3000$. (e) One-fermion walk in the symmetric case, with the initial position at 5.

follow the constraint for the symmetrized case.[8] Subsequently, we can also compute the probability distributions

$$|\langle 1,2|1,2(t)\rangle|^2 = \frac{1}{N^2}[4 + (N-2)^2 + 4(N-2)\cos Nt], \tag{3.14}$$

$$|\langle \psi|1,2(t)\rangle|^2 = \frac{2}{N^2}(1-\cos Nt). \tag{3.15}$$

Here $|\psi\rangle$ denotes the allowed two-fermion states that have an overlap with $|1,2\rangle$. These expressions present a clear indication of the localization for large N as the term $\frac{1}{N^2}[4 + (N-2)^2]$ in (3.14) tends to 1 and the term $\frac{2}{N^2}$ in (3.15) approaches 0.

[8]A similar result for quantum walks on Cayley graphs of the symmetric group is in [62].

C. *k*-fermion walks

This constraining feature continues to hold true for the amplitudes and the corresponding probability distributions in a general k-fermion sector. We will see below that a point in k-dimensional space occupied by k fermions moves to points where at least $k-1$ of the coordinates coincide with the initial state. As in the two-fermion case, this becomes apparent when we work with $\frac{(N-1)!}{(k-1)!(N-k)!}$ eigenstates of the form

$$|[i_1 i_2 \cdots i_{k-1}]\rangle_k = \frac{1}{\sqrt{N-k+1}} a_{i_1}^\dagger a_{i_2}^\dagger \cdots a_{i_{k-1}}^\dagger \times \sum_{\substack{j=1 \\ j\neq\{i_1,i_2,\ldots,i_{k-1}\}}}^{N} a_j^\dagger |\Omega\rangle, \tag{3.16}$$

with $i_1 < i_2 < \cdots < i_{k-1} \in \{1, \ldots, N-1\}$. The second set of eigenstates[9] accounts for $\frac{(N-1)!}{k!(N-k-1)!}$ of them and takes the form

$$|[i_1 i_2 \cdots i_k N]\rangle_k = \frac{1}{\sqrt{k+1}}[a^\dagger_{i_1} \cdots a^\dagger_{i_k} + (-1)^k a^\dagger_{i_2} \cdots a^\dagger_N + \cdots + (-1)^{k^2} a^\dagger_N \cdots a^\dagger_{i_{k-1}}]|\Omega\rangle. \quad (3.17)$$

An initial state of the form $|1, 2, \ldots, k\rangle$ can be expanded using the above eigenstates such that each of them contain at least $k-1$ of $\{1, 2, \ldots, k\}$. Finally, the probability distribution for the time-evolved k-fermion state to overlap with its initial state is

$$|\langle 1, 2, 3, \ldots, k|1, 2, 3, \ldots, k(t)\rangle|^2 = \frac{1}{N^2}[k^2 + (N-k)^2 + 2k(N-k)\cos Nt], \quad (3.18)$$

generalizing the result in (3.14). It is clear from this expression that the localization feature continues to hold for the k-fermion states as well.

IV. DISCUSSION

We have explored the question of localization in a system with superselection sectors and a global discrete symmetry. We saw that in a fermionic system with a global $\mathcal{S}_N$ symmetry, all the basis states of the many-fermion Hilbert space completely localize at all times t for large N. We can understand this result in more general terms as follows. Consider a finite-dimensional quantum system parametrized by the tuples $\lambda_j = \{N, \theta, k, \ldots\}$ with the dimension of the Hilbert space being a function of the integer N. The θ's can be taken as complex in general and the k's could denote another set of integers. The j's index the eigenvalues which, for a system with huge degeneracies, are expected to be much smaller than the size of the Hilbert space. Furthermore, there could be even more parameters denoted by the ellipsis, but for the examples we will consider here these three sets will suffice. We expect such parameters to appear in the Hamiltonian describing the evolution of such quantum systems.

For example, the fully symmetric Hamiltonian (2.15) considered in this paper is only parametrized by N and that presents the only scale for this system. Other systems with lesser and no symmetries will include more parameters. In all such systems the probability distributions are computed using the overlaps

$$\langle\psi|\psi(t)\rangle = \sum_j |c_{\lambda_j}|^2 e^{-iE_{\lambda_j}t}, \quad (4.1)$$

where the E'_{λ_j}s are the energy eigenvalues parametrized by the λ'_js. The normalization factors in the system are expected to go as $O(\frac{1}{N})$ and this is carried over to the coefficients $|c_{\lambda_j}|^2$. The structure of the coefficients will determine the scaling of these overlaps for large N. In the case where N appears as the lone parameter in the system, the degeneracies of the eigenvalues will determine the localization properties. We do not expect to see localization if the number of eigenvalues is $O(N)$ or the degeneracies are $O(1)$. On the other hand, when there are very few eigenvalues, with some of them having degeneracies $O(N)$, we will certainly see localization.

This is precisely the scenario for the $\mathcal{S}_N$-symmetric system studied earlier. When the system includes more parameters, the coefficients c_{λ_j} will also depend on them. In such cases these parameters can be modulated to determine the localization properties for fixed values of N. The energy eigenvalues only appear in the phases of the oscillating terms and are thus not affected at large N.

We will explore such scenarios in this section, which will show that this type of localization can occur in more general systems than the highly symmetric case studied earlier. Furthermore, we also propose a prescription for this type of disorder-free localization. To this end we will elaborate on the following points that will help construct other systems that show a similar phenomenon of disorder-free localization.

(i) We consider including perturbations that break the global $\mathcal{S}_N$ symmetry. We will discuss the cases when localization persists and when it is destroyed.

(ii) We examine the sensitivity of the system to initial conditions. Does the superposition of basis elements of each number sector also show localization? This is another possibility that can affect the coefficients $|c_{\lambda_j}|$. Here again we will see under what conditions localization survives and which states delocalize.

(iii) We look at the role played by the symmetries in the localization. Is this localization only true for fermionic systems? Do spin chains and bosonic systems with global $\mathcal{S}_N$ symmetry also exhibit this type of disorder-free localization? Do the localization features continue to hold for models with reduced global symmetry, namely, $\mathcal{S}_{N-k}$?

(iv) We suggest a plausible prescription by noting a connection between graph theory and the disorder-free localization studied here.

A. Effect of perturbations

The fully symmetric model features localization at large N and for all times t. Naively, we expect a generic perturbation, which breaks the global $\mathcal{S}_N$ symmetry, to make the system delocalize at large times t. We now study the effects of symmetry-breaking perturbations for our system by considering the inclusion of two types of terms: terms that are local and terms that are global with respect to the conjugate variables. More precisely, by local we mean that the number of additional terms is much lower than $O(N)$ and by global we mean that the number of terms we include spans the full range of the conjugate variable, i.e., N. In the global case we find that the system can both localize and delocalize depending on the coefficients appearing in the perturbation, while in the local case the system always stays localized.

1. Case 1

We assume perturbations of the forms $A^\dagger_\alpha A_\beta, A^\dagger_{\alpha_1} A^\dagger_{\alpha_2} A_{\beta_1} A_{\beta_2}$, and higher-order terms. For specific values of the conjugate indices α and β these terms are clearly nonlocal in the real-space indices i, j, k, etc., and they break the global $\mathcal{S}_N$ symmetry. For the first case we keep the number of such terms to be lower than $O(N)$. They commute with the original

[9]The proof for this is in Appendix D.

TABLE I. The one-particle spectrum of (4.2).

Eigenvalue	Eigenstate	Degeneracy
$N-1$	$A_N^\dagger\|\Omega\rangle$	1
-1	$A_\gamma^\dagger\|\Omega\rangle,\ \gamma\neq\alpha,\beta,N$	$N-3$
$\|\theta\|-1$	$\frac{1}{\sqrt{2\|\theta\|}}[\sqrt{\theta}A_\alpha^\dagger+\sqrt{\theta^*}A_\beta^\dagger]\|\Omega\rangle$	1
$-\|\theta\|-1$	$\frac{1}{\sqrt{2\|\theta\|}}[-\sqrt{\theta}A_\alpha^\dagger+\sqrt{\theta^*}A_\beta^\dagger]\|\Omega\rangle$	1

Hamiltonian and hence they introduce only a small split in the energy levels. In particular, the energy levels of, say, the k-particle sector will split into two groups centered around the eigenvalues $-k$ and $N-k$ and with further splits in each group. As a simple example consider the Hamiltonian

$$H_\theta = NA_N^\dagger A_N - \hat{N} + \theta A_\alpha^\dagger A_\beta + \theta^* A_\beta^\dagger A_\alpha, \quad \alpha\neq\beta\neq N. \tag{4.2}$$

The spectrum splits around the unperturbed energy eigenvalues and this is shown for the one-fermion and k-fermion sectors in Tables I and II. In these cases the localization of the basis states for all times continues to hold for any value of the interaction coefficients.

The probability amplitude for the time 0 state $|i\rangle := a_i^\dagger|\Omega\rangle$ to be still in $|i\rangle$ after a time t is found to be

$$\begin{aligned}\langle i|i(t)\rangle = \frac{1}{N}\Bigg[&(N-3)e^{it} + e^{-i(N-1)t} \\ &+ 2\cos^2\left(\frac{\pi}{N}(\beta-\alpha)+\frac{\phi}{2}\right)e^{-i(|\theta|-1)t} \\ &+ 2\sin^2\left(\frac{\pi}{N}(\beta-\alpha)+\frac{\phi}{2}\right)e^{i(|\theta|+1)t}\Bigg],\end{aligned} \tag{4.3}$$

with ϕ the phase factor of the complex number θ. An analogous computation for the k-particle sector of (4.2) gives

$$\begin{aligned}\langle i_1\cdots i_k|i_1\cdots i_k(t)\rangle = \frac{1}{\binom{N}{k}}\left[\binom{N-3}{k}+\binom{N-3}{k-2}\right]e^{ikt} \\ + O\left(\frac{1}{N}\right).\end{aligned} \tag{4.4}$$

TABLE II. The k-particle spectrum of (4.2).

Eigenvalue	Eigenstate	Degeneracy
$N-k$	$A_N^\dagger A_{\gamma_1}^\dagger\cdots A_{\gamma_{k-1}}^\dagger\|\Omega\rangle$	$\binom{N-3}{k-1}$
$N-k$	$A_N^\dagger A_\alpha^\dagger A_\beta^\dagger A_{\gamma_1}^\dagger\cdots A_{\gamma_{k-3}}^\dagger\|\Omega\rangle$	$\binom{N-3}{k-3}$
$N-k+\|\theta\|$	$\frac{1}{\sqrt{2\|\theta\|}}A_N^\dagger[\sqrt{\theta}A_\alpha^\dagger+\sqrt{\theta^*}A_\beta^\dagger]A_{\gamma_1}^\dagger\cdots A_{\gamma_{k-2}}^\dagger\|\Omega\rangle$	$\binom{N-3}{k-2}$
$N-k-\|\theta\|$	$\frac{1}{\sqrt{2\|\theta\|}}A_N^\dagger[-\sqrt{\theta}A_\alpha^\dagger+\sqrt{\theta^*}A_\beta^\dagger]A_{\gamma_1}^\dagger\cdots A_{\gamma_{k-2}}^\dagger\|\Omega\rangle$	$\binom{N-3}{k-2}$
$-k$	$A_{\gamma_1}^\dagger\cdots A_{\gamma_k}^\dagger\|\Omega\rangle$	$\binom{N-3}{k}$
$-k$	$A_\alpha^\dagger A_\beta^\dagger A_{\gamma_1}^\dagger\cdots A_{\gamma_{k-2}}^\dagger\|\Omega\rangle$	$\binom{N-3}{k-2}$
$\|\theta\|-k$	$\frac{1}{\sqrt{2\|\theta\|}}[\sqrt{\theta}A_\alpha^\dagger+\sqrt{\theta^*}A_\beta^\dagger]A_{\gamma_1}^\dagger\cdots A_{\gamma_{k-1}}^\dagger\|\Omega\rangle$	$\binom{N-3}{k-1}$
$-\|\theta\|-k$	$\frac{1}{\sqrt{2\|\theta\|}}[-\sqrt{\theta}A_\alpha^\dagger+\sqrt{\theta^*}A_\beta^\dagger]A_{\gamma_1}^\dagger\cdots A_{\gamma_{k-1}}^\dagger\|\Omega\rangle$	$\binom{N-3}{k-1}$

TABLE III. The k-particle spectrum of (4.5).

Eigenvalue	Eigenstate	Degeneracy
$N-k$	$A_N^\dagger A_{\gamma_1}^\dagger\cdots A_{\gamma_{k-1}}^\dagger\|\Omega\rangle$	$\binom{N-3}{k-1}$
$N-k$	$A_N^\dagger A_\alpha^\dagger A_{\gamma_1}^\dagger\cdots A_{\gamma_{k-2}}^\dagger\|\Omega\rangle$	$\binom{N-3}{k-2}$
$N-k$	$A_N^\dagger A_\beta^\dagger A_{\gamma_1}^\dagger\cdots A_{\gamma_{k-2}}^\dagger\|\Omega\rangle$	$\binom{N-3}{k-2}$
$N-k+\theta$	$A_N^\dagger A_\alpha^\dagger A_\beta^\dagger A_{\gamma_1}^\dagger\cdots A_{\gamma_{k-3}}^\dagger\|\Omega\rangle$	$\binom{N-3}{k-3}$
$-k$	$A_{\gamma_1}^\dagger\cdots A_{\gamma_k}^\dagger\|\Omega\rangle$	$\binom{N-3}{k}$
$-k$	$A_\alpha^\dagger A_{\gamma_1}^\dagger\cdots A_{\gamma_{k-1}}^\dagger\|\Omega\rangle$	$\binom{N-3}{k-1}$
$-k$	$A_\beta^\dagger A_{\gamma_1}^\dagger\cdots A_{\gamma_{k-1}}^\dagger\|\Omega\rangle$	$\binom{N-3}{k-1}$
$\theta-k$	$A_\alpha^\dagger A_\beta^\dagger A_{\gamma_1}^\dagger\cdots A_{\gamma_{k-2}}^\dagger\|\Omega\rangle$	$\binom{N-3}{k-2}$

It is easily verified that the binomial coefficient in (4.6) goes to unity in the large-N limit and this is precisely the signature of localization as seen in the fully $\mathcal{S}_N$-symmetric case.

2. Quartic interaction

Up to now, we have considered only perturbations which are quadratic in the creation and annihilation operators. Now let us introduce a quartic interaction which modifies the Hamiltonian to

$$H_\theta = NA_N^\dagger A_N - \hat{N} + \theta A_\alpha^\dagger A_\beta^\dagger A_\beta A_\alpha, \quad \alpha\neq\beta\neq N. \tag{4.5}$$

As before, this interaction, which is seemingly local in the conjugate variables α, becomes global in the original indices labeled by the j's and also breaks the global $\mathcal{S}_N$ symmetry. The addition of this term affects every $k\geqslant 2$ particle sector. The spectral information in an arbitrary sector can easily be extracted and is listed in Table III. The probability amplitude for the k-particle sector of (4.5) gives

$$\begin{aligned}\langle i_1\cdots i_k|i_1\cdots i_k(t)\rangle = \frac{1}{\binom{N}{k}}\left[\binom{N-3}{k}+2\binom{N-3}{k-1}\right]e^{ikt} \\ + O\left(\frac{1}{N}\right).\end{aligned} \tag{4.6}$$

In the large-N limit, the modulus goes to unity and therefore the state localizes. Thus these perturbations that break the global $\mathcal{S}_N$ symmetry do not spoil the localization features of the fully symmetric system. This continues to hold as long as the number of such perturbations is not too large or is much lower than $O(N)$ and breaks down when the number of terms is comparable to N. This brings us to the second case.

3. Case 2

For the second case we continue including similar interactions as in the first case but now the number of such terms included are $O(N)$. For example, $\sum_{\alpha=1}^N \epsilon_\alpha A_\alpha^\dagger A_\alpha$ is one such simple term. We see that such terms do not disturb the eigenstates and the energy levels continue to split into two groups as long as the perturbation coefficients ϵ_α are not comparable to N. Assuming this is the case, the split is much finer compared to the previous situation and hence the degeneracy is drastically reduced and is no longer $O(N)$ when the ϵ_α's are all unequal. However, if a significant number of ϵ_α's are equal to

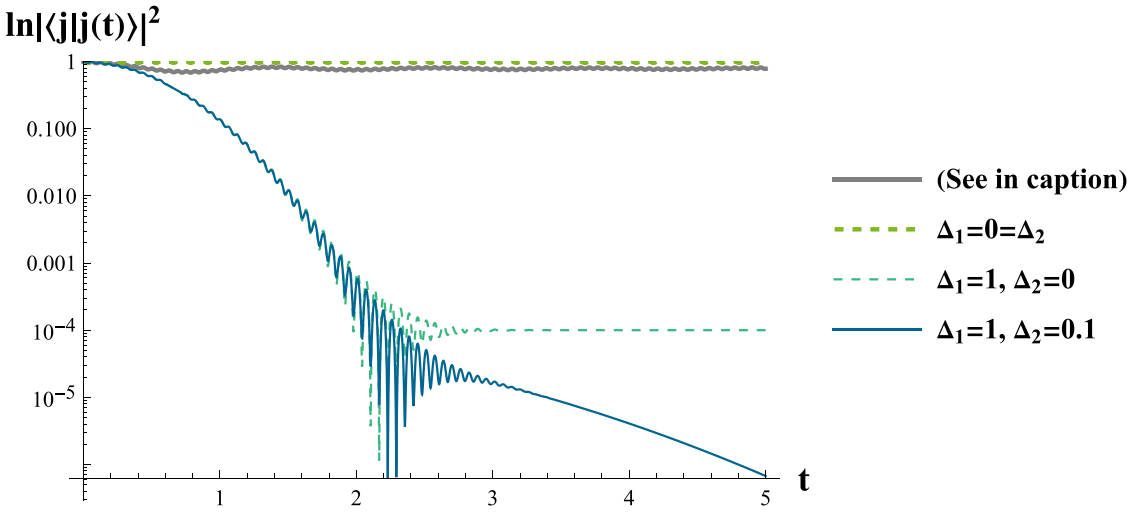

FIG. 2. Plot of the probability distribution $\ln|\langle j|j(t)\rangle|^2$ in the one-particle sector for $N = 100$ with energy splitting as given in case 2. The thick gray curve represents the case where 90 out of the 100 eigenvalues are shifted by an equal amount of 1 and the remaining 10 eigenvalues are shifted by amounts $2\sqrt{l}$ ($l = 1, 2, \ldots, 10$). The other three curves follow from the expression (4.8) with specific values of Δ_1 and Δ_2 as prescribed in the figure. As discussed below, this also can be thought of as representing the behavior of the spectral form factor.

each other we expect to see a different behavior. We will now illustrate both these situations.

We consider the case $G \gg \Delta$, where Δ is a measure of the energy splitting caused by the perturbation and G is the degeneracy before the splitting. Further, we demand that no two energy levels occupy the same energy. Now, owing to the presence of a large number of eigenstates within a very small interval of energy, it is possible to have continuous energy levels and thus an energy distribution function can be associated with them. Also, the distribution function $\rho(E)$ should be such that $\rho(E)|_{\Delta\to 0}$ gives the correct result for the unsplit case. One possible choice can be

$$\rho(E) := \frac{G}{\Delta\sqrt{\pi}} \exp\left(-\frac{(E-E_0)^2}{\Delta^2}\right), \tag{4.7}$$

with E_0 the energy before splitting. The corresponding amplitude in the one-particle sector becomes

$$\langle i|i(t)\rangle = \frac{1}{N^2}[(N-1)e^{it-\Delta_1^2 t^2/4} + e^{-i(N-1+\Delta_2)t}], \tag{4.8}$$

with Δ_1 and Δ_2 the shifts in the energy levels -1 and $N-1$, respectively. In general, for the k-particle sector, we have the expression

$$\langle i_1\cdots i_k|i_1\cdots i_k(t)\rangle = \frac{1}{\binom{N}{k}}\left[\binom{N-1}{k}e^{ikt-\Delta_1^2 t^2/4} + \binom{N-1}{k-1} \times e^{-i(N-k)t-\Delta_2^2 t^2/4}\right], \tag{4.9}$$

where Δ_1 and Δ_2 are the spreads in the energies k and $N-k$, respectively. We show the result graphically in Fig. 2.

In contrast to this, let us consider another situation where we essentially continue working with the previous interaction term, but now the number m of ϵ'_αs assume exactly the same value, with $m \sim O(N)$. As argued earlier, this suggests localization and is further verified by the thick gray plot in Fig. 2.

Interestingly enough, one arrives at identical results while exploring the so-called spectral form factor (SFF), whose behavior is believed to indicate thermalization and chaos in quantum many-body systems [63–65]. The SFF, denoted by $\mathcal{F}(t)$, is defined as

$$\mathcal{F}(t) = \left|\frac{\mathcal{Z}(it)}{\mathcal{Z}(0)}\right|^2, \tag{4.10}$$

where $\mathcal{Z}(\beta + it) = \mathrm{Tr}(e^{-\beta H - iHt})$ is the analytically continued partition function. At $\beta = 0$, the ratio of the partition functions in the k-particle sector becomes

$$\frac{\mathcal{Z}(it)}{\mathcal{Z}(0)} = \frac{\mathrm{Tr}(e^{-iHt})}{\mathrm{Tr}(I)} = \frac{1}{\binom{N}{k}}\sum_\alpha e^{-iE_\alpha t}, \tag{4.11}$$

which, once appropriate energy distributions are chosen, turns out to be exactly the same expression given in (4.9). This happens precisely because the states $|i_1\cdots i_k\rangle$ are equal superpositions of the eigenstates of the Hamiltonian. Therefore, the analysis of the SFF for this particular case can capture the existing features equally well.

Note that we have used number-preserving perturbations and those that commute with the unperturbed Hamiltonian. Perturbations that do not possess these two properties require further investigation.

B. Sensitivity of the system to initial conditions

Using the time-evolution operator in the one-particle sector (see Appendix E), we investigate the sensitivity of the system to the initial conditions by considering an arbitrary initial state $|\psi\rangle = \sum_j c_j|j\rangle$, with $\sum_j |c_j|^2 = 1$. The quantity $|\langle\psi|\psi(t)\rangle|^2$ turns out to be

$$\mathcal{P}(t) := |\langle\psi|\psi(t)\rangle|^2 = 1 - \frac{2\tau(N-\tau)}{N^2}[1-\cos(Nt)], \tag{4.12}$$

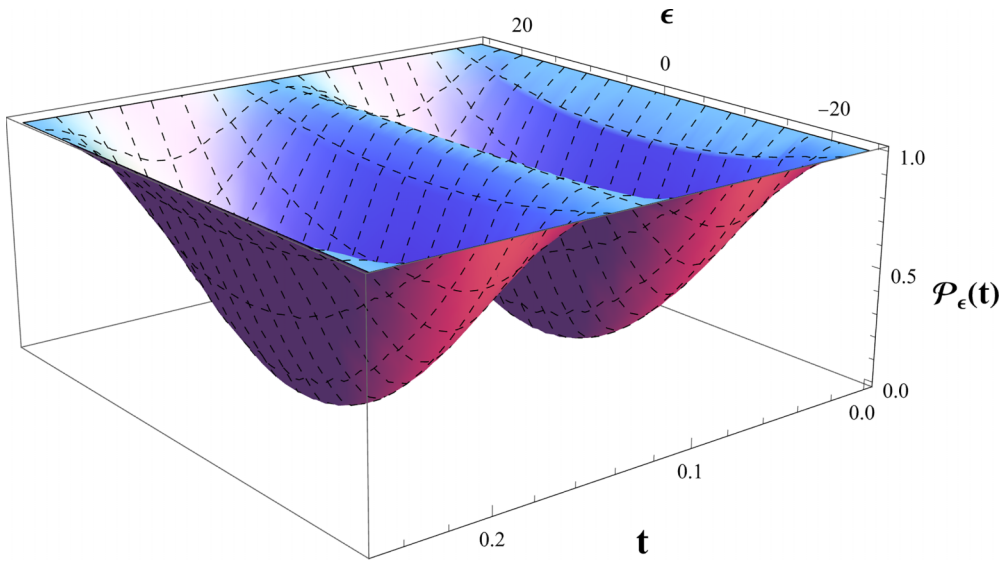

FIG. 3. Plot of $\mathcal{P}_\epsilon(t)$ as a function of ϵ and t ($N = 50$).

where $\tau := \sum_{i,j} \bar{c}_i c_j = \bar{C}C$, with $C := \sum_j c_j$. Evidently, the quantity τ is strictly positive and we can find the maximum value it assumes by the method of Lagrange multipliers. This amounts to solving the system of equations given by $\frac{\partial \tau}{\partial c_i} = \lambda \frac{\partial g}{\partial c_i}$, where $g = \sum_i |c_i|^2 - 1$ and λ is the Lagrange multiplier. The maximum value can be found as $\tau_{\max} = N$.

Note that $\mathcal{P}(t)$ is symmetric about $\tau = N/2$. Around $\tau = \frac{N}{2} + \epsilon$ this becomes

$$\mathcal{P}_\epsilon(t) = \left(\frac{1}{2} + \frac{2\epsilon^2}{N^2}\right) + \left(\frac{1}{2} - \frac{2\epsilon^2}{N^2}\right)\cos(Nt). \tag{4.13}$$

When $\epsilon = 0$ we have $\mathcal{P}_0(t) = \frac{1}{2}[1 + \cos(Nt)]$ and this clearly is not localized. On the other hand, if $\epsilon = \pm\frac{N}{2}$, we find $\mathcal{P}_{\pm N/2}(t) = 1$ and the state is completely localized. In fact, $\tau = N$ corresponds to the eigenstate $|\Phi\rangle = \frac{1}{\sqrt{N}} \sum_i a_i^\dagger |\Omega\rangle$ and $\tau = 0$ corresponds to the eigenstates of the form $|\phi_{[i,j]}\rangle = \frac{1}{\sqrt{2}}(a_i^\dagger - a_j^\dagger)|\Omega\rangle$. If we plot $\mathcal{P}_\epsilon(t)$ as a function of both ϵ and t, we obtain the plot in Fig. 3. One can see for $\epsilon \sim \pm\frac{N}{2}$ the probability remains very close to unity, i.e., the corresponding states are localized, whereas near $\epsilon = 0$ the probability oscillates with time from zero to unity, suggesting that those states are not localized at all.

The result given by (4.12) is also valid for the case of the generic k-particle sector. The quantity τ turns out to be some complicated combination of the coefficients c, appearing in the expansion of the state $|\Psi\rangle$ in the basis $|i_1 \cdots i_k\rangle$. The phenomenon of localization continues to depend on the quantity τ in the same way as in the case of the one-particle sector.

C. Role of symmetries in the localization

It is important to understand the source of the localization and the role played by the two symmetries, i.e., the superselected symmetry and the global $\mathcal{S}_N$ symmetry, in obtaining this feature. To this end we consider the following possibilities.

(1) We examine systems with reduced global symmetry $\mathcal{S}_{N-k}$. We analyze the $k = 1$ case in full detail and then consider the general k case. We find that all these systems localize in a manner similar to the fully symmetric case, implying that the global $\mathcal{S}_N$ symmetry, though sufficient, is not necessary to obtain these localization features.

(2) Next we check if this feature is exclusive to fermionic systems and to verify this we find similar localization features in a spin chain system with global $\mathcal{S}_N$ symmetry and also in $\mathcal{S}_N$-symmetric bosonic systems.

1. Models with reduced global symmetry $\mathcal{S}_{N-1}$

In the first situation we continue working with fermionic systems and reduce the explicit global $\mathcal{S}_N$ symmetry. This is done by identifying a single site, say, 1, to modify the Hamiltonian in (2.15) to

$$H = \beta \sum_{j=2}^{N} [a_1^\dagger a_j + a_j^\dagger a_1] + \sum_{\substack{j,k=2^N \\ j<k}} [a_k^\dagger a_j + a_j^\dagger a_k]. \tag{4.14}$$

This model has a global $\mathcal{S}_{N-1}$ symmetry among the sites $\{2, 3, \ldots, N\}$.[10] To analyze the consequences, we rewrite the Hamiltonian in a different fashion. In the one-fermion sector spanned by

$$a_i^\dagger |\Omega\rangle \to |i\rangle := (0, \ldots, \underbrace{1}_{i\text{th position}}, \ldots, 0),$$
$$i = \{1, 2, \ldots, N\}, \tag{4.15}$$

the Hamiltonian becomes an $N \times N$ matrix. However, owing to the residual $\mathcal{S}_{N-1}$ symmetry, we further can reduce the

[10]These models can be related to central spin systems [66–68] when the unmarked sites are not interacting with each other. These Hamiltonians are also related to the adjacency matrices of cone graphs where similar localization features are studied [69,70] (see Sec. IV D for the connection to graph theory).

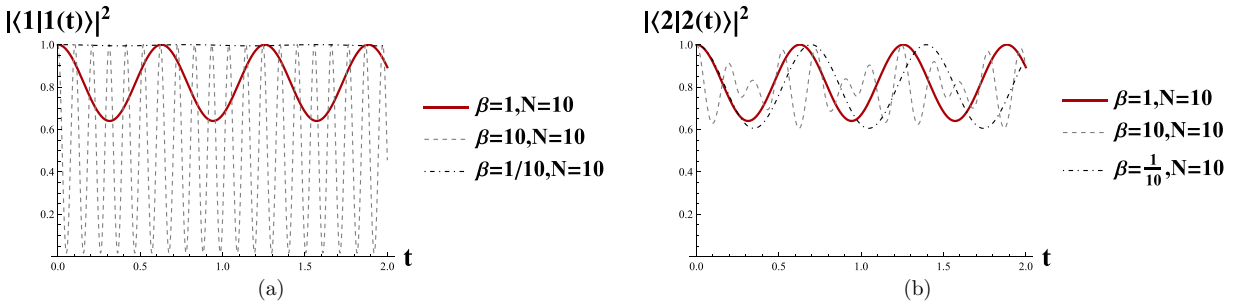

FIG. 4. Probability distributions for the one-fermion sector of (4.14) where the first site is marked: (a) $|\langle 1|1(t)\rangle|^2$ vs t and (b) $|\langle 2|2(t)\rangle|^2$ vs t. The $\beta = 1$ curves correspond to the fully symmetric case and are the same in both (a) and (b). The first particle can now be localized for even small values for N by tuning β appropriately [$\beta = \frac{1}{10}$ curve of (a)]. The other sites with the $\mathcal{S}_{N-1}$ symmetry will be localized for large N. When β is comparable to the value of N ($\beta = N$ curves) we do not see localization.

dimension of the matrix. For example, we can work in the space spanned by

$$\left\{|1\rangle, |2\rangle, \frac{1}{\sqrt{N-2}}(|3\rangle + \cdots + |N\rangle)\right\}. \tag{4.16}$$

The resulting Hamiltonian is

$$H = \begin{pmatrix} 0 & \beta & \beta\sqrt{N-2} \\ \beta & 0 & \sqrt{N-2} \\ \beta\sqrt{N-2} & \sqrt{N-2} & N-3 \end{pmatrix}. \tag{4.17}$$

Using this, the probability that after evolving $|1\rangle$ in time we still find it at $|1\rangle$ becomes

$$|\langle 1|1(t)\rangle|^2 = 1 - \frac{2(N-1)\beta^2\{1-\cos[t\sqrt{(N-2)^2+4(N-1)\beta^2}]\}}{(N-2)^2+4(N-1)\beta^2}. \tag{4.18}$$

Similarly, we can compute $|\langle 2|2(t)\rangle|^2$, and we show the plots for both of these in Figs. 4(a) 4(b). The essential difference between these two is that we can localize $|1\rangle$ even for small N by tuning β, which is not possible for the other states that continue to localize for large-N values as in the case of the full global $\mathcal{S}_N$ symmetry.

2. *Models with reduced global symmetry $\mathcal{S}_{N-k}$*

We expect similar statements to be true for a system with a global $\mathcal{S}_{N-k} \subset \mathcal{S}_N$ symmetry where k points are marked. Consider the oscillators indexed by the conjugate variables α,

$$A_\alpha = \frac{1}{\sqrt{N-k+\sum_{j=1}^k |\theta_j|^2}}\left(\sum_{j=1}^k \omega^{\alpha j}\theta_j a_j + \sum_{j=k+1}^N \omega^{\alpha j} a_j\right), \tag{4.19}$$

TABLE IV. The one-fermion spectrum of the system with reduced global symmetry $\mathcal{S}_{N-k}$.

Eigenvalue	Eigenstate	Degeneracy
1	$A_N^\dagger\|\Omega\rangle$	1
0	$(A_\alpha^\dagger - \kappa_{N\alpha}A_N^\dagger)\|\Omega\rangle,\ \alpha = \{1,\ldots,N-1\}$	$N-1$

with θ_j complex parameters. Using this, the Hamiltonian[11]

$$H = A_N^\dagger A_N \tag{4.20}$$

is a simple example of a system with global $\mathcal{S}_{N-k}$ symmetry. In the original indices, this looks like

$$H = \frac{1}{N-k+\sum_{m=1}^k |\theta_m|^2}\left(\sum_{m,j=1}^k \theta_m^*\theta_j a_m^\dagger a_j + \sum_{m,j=k+1}^N a_m^\dagger a_j + \sum_{m=1}^k\sum_{j=k+1}^N (\theta_m^* a_m^\dagger a_j + \theta_m a_j^\dagger a_m)\right), \tag{4.21}$$

which explicitly reveals the $\mathcal{S}_{N-k}$ global symmetry among the indices $\{k+1,\ldots,N\}$. It is easily verified that oscillators (4.19) satisfy a deformed CAR algebra

$$\begin{aligned} &\{A_\alpha, A_\beta\} = 0 = \{A_\alpha^\dagger, A_\beta^\dagger\}, \\ &\{A_\alpha, A_\alpha^\dagger\} = 1, \\ &\{A_\alpha, A_\beta^\dagger\} = \kappa_{\alpha\beta}, \quad \alpha \neq \beta, \end{aligned} \tag{4.22}$$

with $\kappa_{\alpha\beta} = \frac{\sum_{j=1}^k \omega^{(\alpha-\beta)j}|\theta_j|^2 + \sum_{j=k+1}^N \omega^{(\alpha-\beta)j}}{N-k+\sum_{j=1}^k |\theta_j|^2}$. Note that when the deformation parameters $\theta_j \to 1$, this algebra reduces to the undeformed CAR algebra (3.2). The spectrum of this system is similar to the fully symmetric case as each particle number sector has precisely two eigenvalues. The one-fermion and two-fermion spectra are shown in Tables IV and V, respectively, to illustrate this. We observe that the value of k and the deformation coefficients θ_j do not affect the nature of the spectrum, i.e., they continue to have precisely two eigenvalues for a Hamiltonian taking the form $A_N^\dagger A_N$. We expect the resulting probability distributions to depend on the values of θ_j just as in the $k = 1$ case studied earlier. For example, when

[11]Note that, unlike the Hamiltonian for the $\mathcal{S}_{N-1}$ case, this Hamiltonian also includes the diagonal terms of the form $a_j^\dagger a_j$. Removing them amounts to including the term $\sum_{\alpha=1}^N A_\alpha^\dagger A_\alpha$ in the Hamiltonian. However, unlike the undeformed case, this term does not commute with $A_N^\dagger A_N$ when the oscillators are deformed as in (4.19). This only adds a layer of complication to the computation, but we do not expect the features to change much and so we do not include it here.

TABLE V. The two-fermion spectrum of the system with reduced global symmetry $\mathcal{S}_{N-k}$.

Eigenvalue	Eigenstate	Degeneracy
1	$A_N^\dagger A_\alpha^\dagger\|\Omega\rangle,\ \alpha \neq N$	$N-1$
0	$(A_{\alpha_1}^\dagger A_{\alpha_2}^\dagger - \kappa_{N\alpha_1} A_N^\dagger A_{\alpha_2}^\dagger + \kappa_{N\alpha_2} A_N^\dagger A_{\alpha_1}^\dagger)\|\Omega\rangle,\ \alpha_1 < \alpha_2 \neq N$	$\binom{N-1}{2}$

$j \in \{1, 2, \ldots,\ k\}$ we have, for the time-evolved state,

$$|j(t)\rangle = \frac{1}{N}\left(N + (e^{-it}-1)\sum_{\alpha=1}^{N}\omega^{j\alpha}\kappa_{N\alpha}\right)a_j^\dagger|\Omega\rangle + \frac{1}{N\theta_j^*}\sum_{\substack{l=1\\ l\neq j}}^{k}(e^{-it}-1)\sum_{\alpha=1}^{N}\omega^{j\alpha}\kappa_{N\alpha}\theta_l^* a_l^\dagger|\Omega\rangle$$
$$+ \frac{1}{N\theta_j^*}\sum_{l=k+1}^{N}(e^{-it}-1)\sum_{\alpha=1}^{N}\omega^{j\alpha}\kappa_{N\alpha}a_l^\dagger|\Omega\rangle, \tag{4.23}$$

with normalization $\mathcal{N}$ given by

$$\mathcal{N}^2 = \frac{1}{N^2}\left(N + (e^{-it}-1)\sum_{\alpha_1=1}^{N}\omega^{j\alpha_1}\kappa_{N\alpha_1}\right)\left(N + (e^{it}-1)\sum_{\alpha_2=1}^{N}\omega^{-j\alpha_2}\kappa_{\alpha_2 N}\right)$$
$$+ \frac{1}{N^2|\theta_j|^2}(e^{-it}-1)(e^{it}-1)\sum_{\alpha_1=1}^{N}\omega^{j\alpha_1}\kappa_{N\alpha_1}\sum_{\alpha_2=1}^{N}\omega^{-j\alpha_2}\kappa_{\alpha_2 N}\sum_{\substack{l=1\\ l\neq j}}^{k}|\theta_l|^2$$
$$+ \frac{N-k}{N^2|\theta_j|^2}(e^{-it}-1)(e^{it}-1)\sum_{\alpha_1=1}^{N}\omega^{j\alpha_1}\kappa_{N\alpha_1}\sum_{\alpha_2=1}^{N}\omega^{-j\alpha_2}\kappa_{\alpha_2 N}. \tag{4.24}$$

The apparent time dependence in the above expression should vanish upon simplification, as expected for a unitary system, and we will see this explicitly below. The system with arbitrary complex θ_j's is hard to analyze and so to better understand the behavior of the probability distributions arising from these expressions we make a simplifying assumption that $|\theta_j|^2 = |\theta|^2 > 1$ for all $j \in \{1, 2, \ldots,\ k\}$. This is still a fairly general consideration as the different θ_j's differ in the phases though they have the same magnitude. This simplification makes

$$\kappa_{N\alpha} = \frac{|\theta|^2 - 1}{N + k(|\theta|^2 - 1)}\sum_{j=1}^{k}\omega^{-\alpha j} = \delta\sum_{j=1}^{k}\omega^{-\alpha j}, \tag{4.25}$$

when $\alpha \neq N$. Using this, we see that the frequently occurring sum simplifies as

$$\sum_{\alpha=1}^{N}\omega^{\alpha j}\kappa_{N\alpha} = \begin{cases} 1 + (N-k)\delta & \text{for } j \in \{1, 2, \ldots,\ k\} \\ 1 - k\delta & \text{for } j \in \{k+1, \ldots,\ N\}. \end{cases} \tag{4.26}$$

With this the normalization in (4.24) simplifies to one. For $j \in \{1, 2, \ldots,\ k\}$ the different probability distributions are found to be

$$|\langle j|j(t)\rangle|^2 = \frac{\{N + (e^{-it}-1)[1 + (N-k)\delta]\}\{N + (e^{it}-1)[1 + (N-k)\delta]\}}{N^2}, \tag{4.27}$$

$$|\langle l|j(t)\rangle|^2 = \frac{(e^{-it}-1)(e^{it}-1)[1 + (N-k)\delta]^2}{N^2}, \quad l \in \{1, 2, \ldots, k\},\ l \neq j, \tag{4.28}$$

$$|\langle m|j(t)\rangle|^2 = \frac{(e^{-it}-1)(e^{it}-1)[1 + (N-k)\delta]^2}{N^2|\theta|^2}, \quad m \in \{k+1, \ldots, N\}. \tag{4.29}$$

It is easily seen that the sum of (4.27) and $k-1$ times (4.28) and $N-k$ times (4.29) is one, implying probability conservation, and this serves as a consistency check of our expressions. From these expressions it is clear that for large enough N when compared to θ, only the expression in (4.27) goes to one while the expressions in (4.28) and (4.29) go to zero, implying localization. Furthermore, as in the $\mathcal{S}_{N-1}$ case, with the introduction of the deformation parameters θ, we see that we can now achieve localization by tuning their values for fixed N and k. This is shown in Fig. 5(a), where for $N = 20$

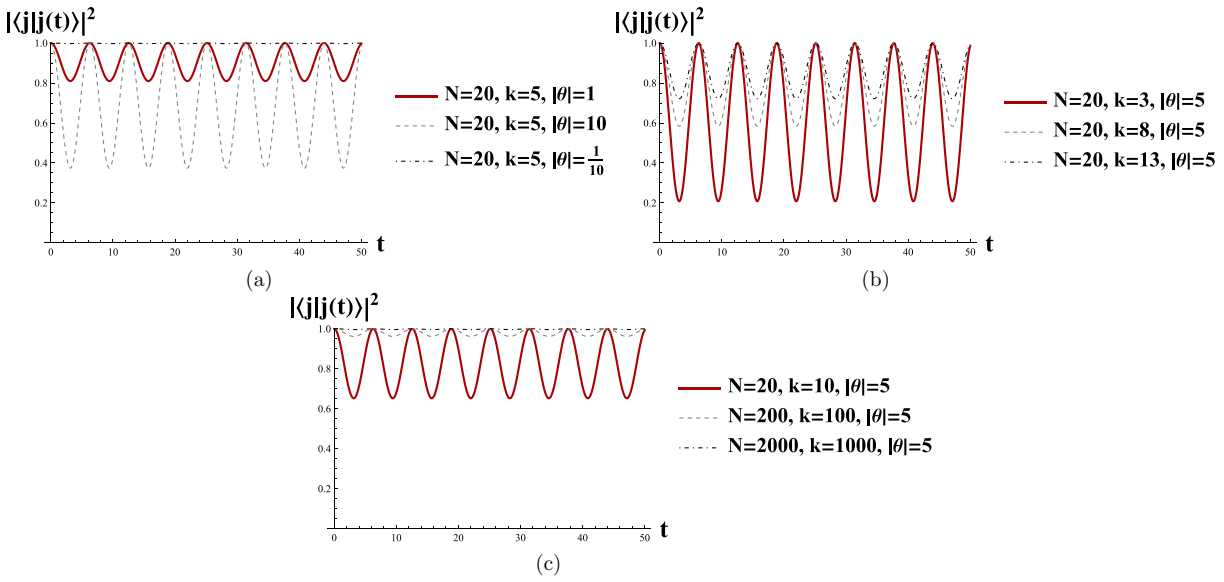

FIG. 5. Probability distribution $|\langle j|j(t)\rangle|^2$, as given by (4.27), plotted as a function of t for different values of (a) θ and (b) k and (c) for different k and N values with fixed $|\theta|$ such that a particular $\frac{k}{N}$ ratio (here 0.5) is maintained. One can arrive at both localization and delocalization by modifying θ and k suitably just as in the $\mathcal{S}_{N-1}$ case studied earlier. Large values of N, with $\frac{k}{N}$ fixed and finite, favor localization as seen in (c).

we obtain almost perfect localization when $\theta = 0.1$, which should be contrasted with the $\theta = 10$ case shown in the same figure.

Note that for $\theta = 1$ the deformed CAR algebra in (4.22) reduces to the undeformed one in (3.2). However, this is still not the fully symmetric case due to the continued presence of the phases in front of the k oscillators. Nevertheless, the probability distributions are blind to these relative phases and hence the answers we obtain in this case are precisely the same as the undeformed or the fully symmetric case. This suggests that the fully deformed model, devoid of any global symmetry and built using the oscillators

$$A_\alpha = \frac{1}{|\theta|\sqrt{N}} \sum_{j=1}^{N} \omega^{\alpha j} \theta_j a_j, \tag{4.30}$$

should mimic the undeformed and fully symmetric case. It is easily seen that the deformed CAR algebra (4.22) reduces to the undeformed one (3.2) for these oscillators. In fact, the probability distributions in this case,

$$|\langle j|j(t)\rangle|^2 = \frac{1}{N^2}(N + e^{it} - 1)(N + e^{-it} - 1), \tag{4.31}$$

$$|\langle l|j(t)\rangle|^2 = \frac{1}{N^2}(e^{it} - 1)(e^{-it} - 1), \quad l \neq j, \tag{4.32}$$

coincide precisely with the undeformed case. These expressions can also be obtained by setting $|\theta| = 1$ or $\delta = 0$ and $k = N$ in (4.27) and (4.28). This is another example where a model without global symmetries localizes in exactly the same way as a model with one, as long as all the fermions interact with each other modulo relative phase coefficients.

The role of k in $\mathcal{S}_{N-k}$ is studied in Fig. 5(b), where we see that for fixed N and $|\theta|$ the system localizes as $k \to N$. Thus the tuning of k can also be used to obtain localization for small N. Moreover, as we increase k and N such that $\frac{k}{N}$ is fixed we see that localization occurs only for large N when $|\theta|$ is fixed [see Fig. 5(c)]. In this case localization for smaller values of N can be obtained by modulating $|\theta|$. Also when $\frac{k}{N} \to 1$ we will always see localization.

As a further extension we remark that Hamiltonians of the form $A_\alpha^\dagger A_\alpha$, diagonal in the conjugate space, will have spectral features similar to those of the fully symmetric case, for both deformed and nondeformed oscillators. These systems do not have any obvious global symmetries in the spaces indices j but feature interactions where all the fermions interact with one another, with some coefficients. We expect all of them to exhibit similar disorder-free localization features.

3. *Spin chain with global $\mathcal{S}_N$ symmetry*

To examine the role of the superselected symmetry, consider a spin chain system with no superselected symmetry and just a global $\mathcal{S}_N$ symmetry. The permutation operator on $\mathbb{C}^2 \otimes \mathbb{C}^2$ can be written using Pauli matrices as

$$\frac{1 + X \otimes X + Y \otimes Y + Z \otimes Z}{2} = \begin{pmatrix} 1 & 0 & 0 & 0 \\ 0 & 0 & 1 & 0 \\ 0 & 1 & 0 & 0 \\ 0 & 0 & 0 & 1 \end{pmatrix}. \tag{4.33}$$

Thus we can generate the full permutation group $\mathcal{S}_N$ using these transpositions as generators. We have

$$s_i \equiv s_{i,i+1} = \frac{1 + X_i X_{i+1} + Y_i Y_{i+1} + Z_i Z_{i+1}}{2} \tag{4.34}$$

as the generators of $\mathcal{S}_N$ and they satisfy (2.5). Well-known spin chains such as the Heisenberg XXX spin chain $H = \sum_{j=1}^{N-1}[X_j X_{j+1} + Y_j Y_{j+1} + Z_j Z_{j+1}]$ is a sum of such operators up to a constant term. For our purposes we use these generators to construct permutation-invariant spin chains using the

TABLE VI. The two-particle spectrum of (2.15) in the bosonic case.

Eigenvalue	Eigenstate	Degeneracy
-2	$A^\dagger_\alpha A^\dagger_\beta \lvert\Omega\rangle,\ \alpha,\beta \neq N$	$\binom{N-1}{2}+N-1$
$2N-2$	$(A^\dagger_N)^2\lvert\Omega\rangle$	1
$N-2$	$A^\dagger_\alpha A^\dagger_N\lvert\Omega\rangle$	$N-1$

techniques of Sec. II. By noting that the generators are just transpositions or 2-cycles, we can express an arbitrary 2-cycle (ij) as a product of the s_i's in (4.34). We have

$$(ij)=\frac{1+X_iX_j+Y_iY_j+Z_iZ_j}{2}, \tag{4.35}$$

where X_i, Y_i, and Z_i are the Pauli matrices on site i. This operator exchanges the states on sites i and j. In this case the two-cycle Hamiltonian generalizes the Heisenberg XXX spin chain[12]

$$H=\frac{1}{2}\sum_{\substack{j,k=1\\ j<k}}^{N}(X_jX_k+Y_jY_k+Z_jZ_k)+\frac{N(N-1)}{2}. \tag{4.36}$$

The two-cycle Hamiltonian is just the sum of the $\frac{N(N-1)}{2}$ transpositions acting on $\otimes_{j=1}^N\mathbb{C}^2_j$. We will call this the symmetric Heisenberg XXX spin chain.

The Hilbert space of this system splits into sectors labeled by the number of $|\downarrow\rangle'$s, as the Hamiltonian, being the sum of permutation operators, cannot mix states containing different numbers of $|\downarrow\rangle'$s. Thus the problem we have now is similar to the one encountered in the fermionic realization. For example, consider the sector where there is a single $|\downarrow\rangle$ with the remaining sites filled by a $|\uparrow\rangle$. There are N such states and the Hamiltonian in this sector reduces to the form

$$(H_1)_{ij}=\left(\frac{(N-1)(N-2)}{2}-1\right)\delta_{ij}+1, \tag{4.37}$$

which is similar to the one obtained in the fermion case (E1) modulo the function of N appearing with the δ_{ij}. We expect to see localization here as well, suggesting that this property is true regardless of the realization chosen for the global permutation symmetry. It is not hard to see that this pattern continues for the other sectors of this Hilbert space and so we conclude that the symmetric XXX chain of (4.36) will contain localized states for large N.

4. Bosonic systems with global $\mathcal{S}_N$ symmetry

The symmetric Hamiltonian in (2.15) can also be considered for the bosonic case by merely enforcing the canonical commutation relations for the operators appearing in the Hamiltonian. While the one-particle spectrum of this model is similar to the fermionic case, the spectra of other sectors are different. For the higher-particle-number sectors the number of energy eigenvalues depends on the particle number of the sector. There are $k+1$ energy eigenvalues for the k-particle sector. The spectrum of the two-particle sector is shown in Table VI. The probability for the two-particle basis states is found to be

$$|\langle 1,2|1,2(t)\rangle|^2=\frac{2}{N^4}\left(\frac{1+4(N-1)^2+(N-1)^4}{2}+2(N-1)\cos(E_1-E_2)t+2(N-1)^3\cos(E_2-E_3)t\right.$$
$$\left.+(N-1)^2\cos(E_3-E_1)t\right). \tag{4.38}$$

For large N this expression clearly goes to unity, indicating the same type of disorder-free localization as seen in the fermionic system. The probabilities go as $\frac{1}{N^4}$ and $\frac{1+(N-2)^2+(N-1)^2}{N^4}$ when $|1,2(t)\rangle$ overlaps with $|j,k\rangle$ and $|1,k\rangle$, $|2,k\rangle$, respectively. Similar localization is seen in the higher boson sectors as well and thus we conclude that this type of disorder-free localization is also true for bosonic systems with global $\mathcal{S}_N$ symmetry.

D. Prescription for disorder-free localization using graph theory

We begin with a few definitions from graph theory to keep this part self-contained. A graph $G=(V,E)$ consists of a set of vertices (V) and a set of edges (E). We consider simple and regular graphs, which are those where more than one edge is not allowed between two vertices and where all the vertices have the same valence. The adjacency matrix A of a simple and regular graph is a $|V|\times|V|$ matrix with matrix elements $A_{ij}=1$ when vertices i and j are connected by an edge and $A_{ij}=0$ when they are not.

From the graph theory perspective the Hamiltonian of the one-fermion sector (E1) is precisely the adjacency matrix of a complete graph.[13] The automorphism group of such a graph is precisely $\mathcal{S}_N$, where N is identified as the number of vertices of this graph.

Now we establish the localization features seen in the one-fermion Hamiltonian (E1) for the complete graph. To do this we begin by making the set of vertices into a Hilbert space $\mathbb{C}^N$ with the N basis vectors given by $|j\rangle=(0\cdots1\cdots0)^T$, with 1 at the jth position and the inner product taken as the canonical

[12]The Heisenberg XXX spin chain $H=\sum_{j=1}^{N-1}(X_jX_{j+1}+Y_jY_{j+1}+Z_jZ_{j+1})$ is a local Hamiltonian with nearest-neighbor interactions. This can be thought of as an analog of the tight-binding Hamiltonian. The analog of the $\mathcal{S}_N$-symmetric Hamiltonian in (2.15) is the model given by (4.36).

[13]A complete graph is a simple graph where all vertices are connected with each other.

one. Then the vectors $|j\rangle$ are evolved according to

$$|j(t)\rangle = e^{iAt}|j\rangle. \tag{4.39}$$

Computing the probability corresponding to the overlap $\langle 1|1(t)\rangle$,

$$|\langle 1|1(t)\rangle|^2 = \frac{1}{N^2}[1 + (N-1)^2 + 2(N-1)\cos Nt], \tag{4.40}$$

we see that it coincides with the one-fermion quantum walk expression (3.8). The probability distributions corresponding to states other than $|1\rangle$ precisely coincide with (3.9). These results have appeared in the quantum walk literature from the perspective of algebraic graph theory (see Sec. 1 of [69], Eq. 15 of [71], Eq. 4 of [72], and [73,74]). Such localization properties manifest as sedentariness in continuous-time quantum walks and the "stay-at-home" property in the jargon of graph theory. More generally, graph theorists study strongly regular graphs (SRGs) [75,76] whose adjacency matrices have spectra with the right properties to obtain the stay-at-home property [69]. Strongly regular graphs are characterized by a 4-tuple $(n, k; a, c)$, with n the number of vertices, k the valence, a the number of common neighbors for adjacent vertices, and c the number of common neighbors for nonadjacent vertices. Their adjacency matrices satisfy the characteristic equation [69,75]

$$A^2 - (a-c)A - (k-c)I = cJ, \tag{4.41}$$

where I is the identity matrix of size n and J is the square matrix with all entries unity. This matrix has just three eigenvalues, one of which is nondegenerate and the other two scale with n.

Not all strongly regular graphs exhibit localization, but a particular family characterized by the tuple $(n^2, k(n-1); n-2+(k-1)(k-2), k(k-1))$ does show localization [69]. Most of the strongly regular graphs have trivial automorphism groups [75], which shows that the global symmetry is really not necessary to see this kind of disorder-free localization.

Interpreting the adjacency matrices as many-body Hamiltonians, we see that they only capture the one-particle sectors of the corresponding physical systems. In this paper we have shown how to construct the physical Hamiltonians[14] corresponding to such graphs which facilitate the study of the localization properties of multiparticle sectors as well. For example, the fermionic Hamiltonian corresponding to an adjacency matrix A can be constructed by replacing the matrix elements of A by $a_i^\dagger a_j + a_j^\dagger a_i$ if and only if $A_{ij} = 1$. With this rule, the fermionic Hamiltonian corresponding to the complete graph is precisely the $\mathcal{S}_N$-symmetric model in (2.15). This can then be used to study the higher-fermion sectors. With this algorithm it is only natural to conjecture that the Hamiltonians corresponding to SRGs can be prescribed as a way to obtain the disorder-free localization studied in this paper. We reserve the investigation of this interesting connection for a future work.

[14]Note that in graph theory the localization results are derived purely by studying the characteristic equation which translates to the spectra of the underlying graphs. The exact form of the adjacency matrix is not required to establish localization in graph spectra. In fact, it is a hard problem to construct the adjacency matrices of strongly regular graphs [75].

V. CONCLUSION

We end with a few remarks and possible future works.

(i) The models described in this paper feature all-to-all connectivity of multiple fermions which are essentially two-level systems, implying that they can be realized with qubit systems. The many-fermion Hamiltonians in (2.15), (4.2), and (4.5) can be modeled on both planar and nonplanar architectures depending on the potentials used to realize the interqubit couplings. However, it is in general impractical and hard to engineer such long-range couplings between qubits in experiments. Nevertheless, such systems are important in quantum computing architectures as they can implement different quantum algorithms that assume quantum gates operate on an arbitrary pair of qubits. An implementation of the homogeneous all-to-all connectivity among qubits was proposed in [77] using superconducting qubits in circuit QED. Also, there are now experiments in superconducting circuits using bus resonators that can achieve tunable all-to-all couplings [78,79] and more recently with ring resonators [80]. The architecture proposed in the latter is also scalable and prevents crosstalk between qubits.

All-to-all connectivity can also be seen in digital quantum simulators using trapped ions [81,82]. In these setups the qubits are encoded in the Zeeman states of electrically trapped and laser-cooled calcium ions. A universal set of gates is implemented in this system and they can simulate several types of interactions among the qubits including nonlocal ones apart from the local terms. These experiments also support both inhomogeneous and homogeneous couplings. Similar effects are also seen in ultracold-atom setups [83].

(ii) The out-of-time-order correlators (OTOCs) indicate chaotic behavior in thermal systems [84]. The Lyapunov exponent can be read off from such expressions [24]. The saturation of this quantity implies behavior similar to that predicted by the anti–de Sitter/conformal field theory correspondence and is like an SYK model [22–25]. The systems discussed in this work describe the opposite behavior and thus the results on the OTOCs do not hold for them.

(iii) An extension worthy of mention is adding an internal symmetry index $\alpha = 1, 2$ transforming by the spin-$\frac{1}{2}$ representation of SU(2) to the operators a_i. Then, since this representation is pseudoreal, $a_i^\alpha (\sigma_2)_{\alpha,\alpha'} a_j^{\alpha'}$ is SU(2) invariant and so is its adjoint (here σ_2 is the second Pauli matrix.). So we can add such SU(2) or color singlet Majorana terms which are also permutation invariant and incorporate features of the SYK model.

(iv) Furthermore, it would be interesting to consider the algebra of observables that are permutation invariant and study the corresponding Hilbert spaces built using the Gel'fand-Naimark-Segal construction [85–90]. These can then be used to explore the entanglement entropy and thermalization properties of these systems and those derived from them.

ACKNOWLEDGMENTS

Certain ideas in this paper were initiated in discussions of A.P.B. and Fabio Di Cosmo, which we gratefully acknowledge. A.P.B. gratefully acknowledges The Institute of Mathematical Sciences, Chennai, as well as Ravindran, and Sanatan Digal. A.K. acknowledges support from the Department of Atomic Energy, Government of India, under Project No. RTI4001. A.S. and P.P. thank Tapan Mishra and Abhishek Chowdhury for useful discussions. A.K. and P.P. acknowledge useful comments and suggestions from Sibasish Ghosh. P.P. thanks G. Baskaran and Ayan Mukhopadhyay for useful discussions. P.P. also acknowledges discussions with Kristian Hauser Villegas and Kim Kun Woo. We would also like to thank the anonymous referees for several critical comments that helped improve the paper.

APPENDIX A: $H_1^{(2)}$ IN DIFFERENT PARTICLE SECTORS

Let us consider the operator

$$H_1^{(2)} = \sum_{\substack{\rho\in 2\text{-cycle}\\ \text{conjugacy class}}} \sum_{i=1}^{N} a^\dagger_{\rho(i)} a_i. \tag{A1}$$

This is invariant in every particle sector under global permutations among the site indices. In the one-particle sector this can be seen very easily:

$$\left(\sigma_1 H_1^{(2)} \sigma_1^{-1}\right) a_m^\dagger |\Omega\rangle = H_1^{(2)} a_m^\dagger |\Omega\rangle. \tag{A2}$$

Here σ_1 is the realization of $\sigma \in \mathcal{S}_N$ in the one-particle sector.

However, before proceeding further, let us consider the action of $H_1^{(2)}$ on an arbitrary k-particle state $a^\dagger_{i_1}\cdots a^\dagger_{i_k}|\Omega\rangle$. We can write.

$$\begin{aligned} H_1^{(2)} a^\dagger_{i_1}\cdots a^\dagger_{i_k}|\Omega\rangle &= \sum_{\substack{\rho\in 2\text{-cycle}\\ \text{conjugacy class}}} (a^\dagger_{\rho(i_1)}a_{i_1} + \cdots + a^\dagger_{\rho(m)}a_m + \cdots + a^\dagger_{\rho(i_k)}a_{i_k}) a^\dagger_{i_1}\cdots a^\dagger_{i_k}|\Omega\rangle \quad \text{(rests give 0)} \\ &= \sum_{\substack{\rho\in 2\text{-cycle}\\ \text{conjugacy class}}} (a^\dagger_{\rho(i_1)}\cdots a^\dagger_{i_k} + a^\dagger_{i_1}\cdots a^\dagger_{\rho(m)}\cdots a^\dagger_{i_k} + a^\dagger_{i_1}\cdots a^\dagger_{\rho(i_k)})|\Omega\rangle \end{aligned} \tag{A3}$$

We will now demonstrate the invariance of $H_1^{(2)}$ in the k-particle sector,

$$\begin{aligned} \sigma_k H_1^{(2)} \sigma_k^{-1} |i_1,\ldots,\ i_k\rangle &= \sigma_k H_1^{(2)} |\sigma^{-1}(i_1),\ldots,\sigma^{-1}(i_k)\rangle \\ &= \sigma_k \sum_{\substack{\rho\in 2\text{-cycle}\\ \text{conjugacy class}}} (|\rho\sigma^{-1}(i_1),\ldots,\sigma^{-1}(i_k)\rangle + \cdots + |\sigma^{-1}(i_1),\ldots,\rho\sigma^{-1}(i_k)\rangle) \\ &= \sum_{\substack{\rho\in 2\text{-cycle}\\ \text{conjugacy class}}} (|\sigma\rho\sigma^{-1}(i_1),\ldots,i_k\rangle + \cdots + |i_1,\ldots,\sigma\rho\sigma^{-1}(i_k)\rangle) \\ &= \sum_{\substack{\rho'\in 2\text{-cycle}\\ \text{conjugacy class}}} (|\rho'(i_1),\ldots,i_k\rangle + \cdots + |i_1,\ldots,\rho'(i_k)\rangle) \\ &= H_1^{(2)}|i_1,\ldots,i_k\rangle, \end{aligned} \tag{A4}$$

where $\sigma\rho\sigma^{-1} = \rho' \in$ 2-cycle conjugacy class also and σ_k is the realization of $\sigma \in \mathcal{S}_N$ in the k-particle sector.

APPENDIX B: PROOF OF (2.16)

The quartic Hamiltonian originating from the two-cycle conjugacy class is

$$H_2^{(2)} = \sum_\sigma \sum_{i<j} a^\dagger_{\sigma(i)} a^\dagger_{\sigma(j)} a_j a_i = \tfrac{1}{2}\sum_{i,j}\sum_\sigma a^\dagger_{\sigma(i)} a^\dagger_{\sigma(j)} a_j a_i. \tag{B1}$$

We notice that all σ's belonging to the two-cycle conjugacy class can be grouped as $i \to i$ and $j \to j$ if there are ${}^{N-2}C_2$ such elements, $i \to j$ and $j \to i$ there is one such element, $i \to i$ and $j \to m\,(\neq i, j)$ if there are $N-2$ such elements, and $i \to m\,(\neq i, j)$ and $j \to j$ if there are $N-2$ such elements. Considering this, we can simplify (B1) as

$$H_2^{(2)} = \frac{1}{2}\sum_{i,j}\left({}^{N-2}C_2 a_i^\dagger a_j^\dagger a_j a_i + a_j^\dagger a_i^\dagger a_j a_i + \sum_{m\neq i,j}(a_i^\dagger a_m^\dagger + a_m^\dagger a_j^\dagger) a_j a_i\right). \tag{B2}$$

With $A = \sum_i a_i$, $\hat{N} = \sum_i a_i^\dagger a_i$, the number operator, and using the relations $[\hat{N}, A/a] = -A/a$, we obtain

$$\begin{aligned} H_2^{(2)} &= \frac{1}{2}({}^{N-2}C_2 - 3)(\hat{N}^2 - \hat{N}) + (A^\dagger A\hat{N} - A^\dagger A) \\ &= \frac{1}{2}\left(\frac{(N-2)(N-3)}{2} - 1\right)(\hat{N}^2 - \hat{N}) \\ &\quad + 2\sum_{i<j}[a_i^\dagger a_j + a_j^\dagger a_i](\hat{N} - 1). \end{aligned} \tag{B3}$$

So we can write $H_2^{(2)}$ in terms of $H_1^{(2)}$ and $\hat{N}$ and we expect this trend to continue for higher-order Hamiltonians like a hexatic Hamiltonian and so on.

APPENDIX C: ORTHOGONALITY AND COMPLETENESS OF (3.11) and (3.12)

The inner product between two-fermion eigenstates $\langle u|v\rangle$ is zero when $|u\rangle$ is in (3.11) and $|v\rangle$ is in (3.12). However, when both $|u\rangle$ and $|v\rangle$ belong to any particular eigenvalue they may not be orthogonal to each other. Nevertheless, we can show that these states are complete using the action of the permutation operators from $\mathcal{S}_N$. To do this we first note that the states in (3.11) are mapped onto each other,

$$s_{jk}|[j]\rangle_2 = |[k]\rangle_2, \quad j,k \in \{1,2,\ldots,N-1\}, \tag{C1}$$

using the transpositions s_{jk} and the states in (3.12) are mapped onto each other,

$$s_{j_1 j_2}s_{k_1 k_2}|[j_1 k_1 N]\rangle_2 = |[j_2 k_2 N]\rangle_2, \tag{C2}$$

using the permutations $s_{j_1 j_2}s_{k_1 k_2}$. Combining these identities with the expression of the two-fermion state $|1,2\rangle$ in (3.13), we see that any other two-fermion state $|j,k\rangle$, with $j,k \neq \{1,2\}$, can be obtained as

$$\begin{aligned} |j,k\rangle &= s_{1j}s_{2k}|1,2\rangle \\ &= \frac{\sqrt{N-1}}{N}(|[j]\rangle_2 - |[k]\rangle_2) + \frac{\sqrt{3}(N-2)}{N}|[jkN]\rangle_2 \\ &\quad - \frac{\sqrt{3}}{N}\sum_{m=3}^{N-1}(|[jmN]\rangle_2 - |[kmN]\rangle_2). \end{aligned} \tag{C3}$$

Notice that we have used $s_{1j}|[2]\rangle_2 = |[2]\rangle_2$ and $s_{2k}|[1]\rangle_2 = |[1]\rangle_2$. On the other hand, the states of the form $|1,j\rangle$ and $|2,j\rangle$, for $j \in \{3,\ldots,N\}$, are obtained by applying s_{2j} and s_{1j} on $\pm|1,2\rangle$, respectively. Thus any two-fermion state can be written as a linear combination of the two-fermion eigenstates in (3.11) and (3.12), showing their completeness. These arguments can be extended to a general k-fermion sector as well.

APPENDIX D: PROOF OF (3.17)

We have the action of quadratic all-to-all on a general k-particle state as

$$H_1^{(2)}a_{i_1}^\dagger \cdots a_{i_k}^\dagger|\Omega\rangle = \sum_\sigma (a_{\sigma(i_1)}^\dagger \cdots a_{i_k}^\dagger + a_{i_1}^\dagger \cdots a_{\sigma(i_j)}^\dagger \cdots a_{i_k}^\dagger + \cdots + a_{i_1}^\dagger \cdots a_{\sigma(i_k)}^\dagger)|\Omega\rangle. \tag{D1}$$

We concentrate on the single term $\sum_\sigma a_{i_1}^\dagger \cdots a_{\sigma(i_j)}^\dagger \cdots a_{i_k}^\dagger$. As done previously, we can group the σ's as $i_j \to i_j$ if there are ${}^{N-1}C_2$ such elements and $i_j \to m \neq i_j$ if there are $N-1$ such elements. Then we finally have

$$\begin{aligned} \sum_\sigma a_{i_1}^\dagger \cdots a_{\sigma(i_j)}^\dagger \cdots a_{i_k}^\dagger &= {}^{N-1}C_2\, a_{i_1}^\dagger \cdots a_{i_j}^\dagger \cdots a_{i_k}^\dagger + a_{i_1}^\dagger \cdots \left(\sum_{m\neq i_j} a_m^\dagger\right) \cdots a_{i_k}^\dagger \\ &= ({}^{N-1}C_2 - 1)\, a_{i_1}^\dagger \cdots a_{i_j}^\dagger \cdots a_{i_k}^\dagger + a_{i_1}^\dagger \cdots \left(\sum_m a_m^\dagger\right) \cdots a_{i_k}^\dagger \\ &= ({}^{N}C_2 - N) a_{i_1}^\dagger \cdots a_{i_k}^\dagger + a_{i_1}^\dagger \cdots \underbrace{A^\dagger}_{j\text{th position}} \cdots a_{i_k}^\dagger. \end{aligned} \tag{D2}$$

Therefore, we have

$$H_1^{(2)}a_{i_1}^\dagger \cdots a_{i_k}^\dagger|\Omega\rangle = k({}^{N}C_2 - N)a_{i_1}^\dagger \cdots a_{i_k}^\dagger|\Omega\rangle + A^\dagger a_{i_2}^\dagger \cdots a_{i_k}^\dagger|\Omega\rangle + \cdots + a_{i_1}^\dagger \cdots \underbrace{A^\dagger}_{j\text{th position}} \cdots a_{i_k}^\dagger|\Omega\rangle + \cdots + a_{i_1}^\dagger \cdots a_{i_{k-1}}^\dagger A^\dagger|\Omega\rangle. \tag{D3}$$

Now let us consider the situation

$$\begin{aligned} H_1^{(2)}a_{i_1}^\dagger \cdots \sum_{i_k} a_{i_k}^\dagger|\Omega\rangle &= k({}^{N}C_2 - N)a_{i_1}^\dagger \cdots \sum_{i_k} a_{i_k}^\dagger|\Omega\rangle + A^\dagger a_{i_2}^\dagger \cdots \sum_{i_k} a_{i_k}^\dagger|\Omega\rangle + \cdots \\ &\quad + a_{i_1}^\dagger \cdots \underbrace{A^\dagger}_{j\text{th position}} \cdots \sum_{i_k} a_{i_k}^\dagger|\Omega\rangle + \cdots + a_{i_1}^\dagger \cdots a_{i_{k-1}}^\dagger \sum_{i_k} A^\dagger|\Omega\rangle \\ &= k({}^{N}C_2 - N)a_{i_1}^\dagger \cdots A^\dagger|\Omega\rangle + N a_{i_1}^\dagger \cdots A^\dagger|\Omega\rangle. \end{aligned} \tag{D4}$$

Thus we have the following eigenstates of $H_1^{(2)}$:

$$H_1^{(2)} a_{i_1}^\dagger \cdots A^\dagger |\Omega\rangle = [{}^N C_2 - N(k-1)] a_{i_1}^\dagger \cdots A^\dagger |\Omega\rangle. \tag{D5}$$

Now let us consider another kind of state

$$|i_1, \ldots, i_k, N; k\rangle = a_{i_1}^\dagger \cdots a_{i_k}^\dagger |\Omega\rangle + \cdots + (-1)^{jk} a_{j+1}^\dagger \cdots a_{i_k}^\dagger \underbrace{a_N^\dagger}_{(k-j+1)\text{th position}} a_{i_1}^\dagger \cdots a_{j-1}^\dagger |\Omega\rangle + \cdots + (-1)^{k^2} a_N^\dagger a_{i_1}^\dagger \cdots a_{i_{k-1}}^\dagger |\Omega\rangle. \tag{D6}$$

Let us focus on two particular expressions

$$H_1^{(2)} a_{i_1}^\dagger \cdots a_{i_k}^\dagger |\Omega\rangle, \quad H_1^{(2)} (-1)^{jk} a_{j+1}^\dagger \cdots a_{i_k}^\dagger \underbrace{a_N^\dagger}_{(k-j+1)\text{th position}} a_{i_1}^\dagger \cdots a_{j-1}^\dagger |\Omega\rangle. \tag{D7}$$

We should have two terms coming from the above,

$$a_{i_1}^\dagger \cdots \underbrace{A^\dagger}_{j\text{th position}} \cdots a_{i_k}^\dagger |\Omega\rangle, \quad (-1)^{jk} a_{j+1}^\dagger \cdots a_{i_k}^\dagger \underbrace{A^\dagger}_{(k-j+1)\text{th position}} a_{i_1}^\dagger \cdots a_{j-1}^\dagger |\Omega\rangle. \tag{D8}$$

They have same index content. Rearrangement of the indices in the second of these yields

$$\begin{aligned}(-1)^{(k-j+1)(j-1)+(k-j)+jk} a_{i_1}^\dagger \cdots \underbrace{A^\dagger}_{j\text{th position}} \cdots a_{i_k}^\dagger |\Omega\rangle &= (-1)^{-j^2+2jk+j-1} a_{i_1}^\dagger \cdots \underbrace{A^\dagger}_{j\text{th position}} \cdots a_{i_k}^\dagger |\Omega\rangle \\ &= (-1)^{-j^2+j} (-1)^{2jk-1} a_{i_1}^\dagger \cdots \underbrace{A^\dagger}_{j\text{th position}} \cdots a_{i_k}^\dagger |\Omega\rangle \\ &= -a_{i_1}^\dagger \cdots \underbrace{A^\dagger}_{j\text{th position}} \cdots a_{i_k}^\dagger |\Omega\rangle. \end{aligned} \tag{D9}$$

Thus these terms always cancel and the states $|i_1, \ldots, i_k, N; k\rangle$ are eigenstates of $H_1^{(2)}$:

$$H_1^{(2)} |i_1, \ldots, i_k, N; k\rangle = k({}^N C_2 - N) |i_1, \ldots, i_k, N; k\rangle. \tag{D10}$$

APPENDIX E: TIME EVOLUTION OPERATOR IN THE ONE-PARTICLE SECTOR

The one-particle Hilbert space spanned by $\{a_i^\dagger |\Omega\rangle; i = 1, 2, \ldots, N\}$ can equivalently be described by the space spanned by

$$\{|i\rangle = (0, \ldots, \underbrace{1}_{i\text{th position}}, \ldots, 0)^T\}.$$

In this framework, the bilinear Hamiltonian in (2.15) is given by

$$(H)_{ij} = 1 - \delta_{ij} \Rightarrow H = \mathcal{I} - \mathbb{I}, \tag{E1}$$

where the matrix $\mathcal{I}$ has entries $\mathcal{I}_{ij} = 1$ and the matrix $\mathbb{I}$ is the $N \times N$ identity matrix with entries $\mathbb{I}_{ij} = \delta_{ij}$. They satisfy the properties

$$\mathcal{I}^m = N^{m-1} \mathcal{I}, \quad \mathbb{I}^m = \mathbb{I}. \tag{E2}$$

Then we can simplify

$$e^{-iHt} = \left[\left(\mathbb{I} - \frac{\mathcal{I}}{N} \right) + \frac{\mathcal{I}}{N} e^{-iNt} \right] e^{it}. \tag{E3}$$

The matrix amplitudes turn out to be

$$\langle i | e^{-iHt} | j \rangle = \left[\left(\delta_{ij} - \frac{1}{N} \right) + \frac{1}{N} e^{-iNt} \right] e^{it}. \tag{E4}$$

Further, the probability can be calculated as

$$\begin{aligned} |\langle j | j(t) \rangle|^2 &= \left| \left[\left(1 - \frac{1}{N} \right) + \frac{1}{N} e^{-iNt} \right] e^{it} \right|^2 \\ &= \frac{1}{N^2} [1 + (N-1)^2 + 2(N-1)\cos(Nt)] \end{aligned} \tag{E5}$$

$$\begin{aligned} |\langle j' | j(t) \rangle|^2_{j' \neq j} &= \left| \left(-\frac{1}{N} + \frac{1}{N} e^{-iNt} \right) e^{it} \right|^2 \\ &= \frac{2}{N^2} [1 - \cos(Nt)]. \end{aligned} \tag{E6}$$

[1] P. W. Anderson, Absence of diffusion in certain random lattices, Phys. Rev. **109**, 1492 (1958).

[2] D. M. Basko, I. Aleiner, and B. L. Altshuler, Metal–insulator transition in a weakly interacting many-electron system with localized single-particle states, Ann. Phys. (NY) **321**, 1126 (2006).

[3] M. Srednicki, Chaos and quantum thermalization, Phys. Rev. E **50**, 888 (1994).

[4] J. M. Deutsch, Quantum statistical mechanics in a closed system, Phys. Rev. A **43**, 2046 (1991).

[5] J. M. Deutsch, Eigenstate thermalization hypothesis, Rep. Prog. Phys. **81**, 082001 (2018).

[6] B. Buča, Unified theory of local quantum many-body dynamics: Eigenoperator thermalization theorems, Phys. Rev. X **13**, 031013 (2023).

[7] A. Smith, J. Knolle, D. L. Kovrizhin, and R. Moessner, Disorder-free localization, Phys. Rev. Lett. **118**, 266601 (2017).

[8] A. Smith, J. Knolle, R. Moessner, and D. L. Kovrizhin, Absence of ergodicity without quenched disorder: From quantum disentangled liquids to many-body localization, Phys. Rev. Lett. **119**, 176601 (2017).

[9] M. Brenes, M. Dalmonte, M. Heyl, and A. Scardicchio, Many-body localization dynamics from gauge invariance, Phys. Rev. Lett. **120**, 030601 (2018).

[10] I. Papaefstathiou, A. Smith, and J. Knolle, Disorder-free localization in a simple $U(1)$ lattice gauge theory, Phys. Rev. B **102**, 165132 (2020).

[11] M. Schulz, C. A. Hooley, R. Moessner, and F. Pollmann, Stark many-body localization, Phys. Rev. Lett. **122**, 040606 (2019).

[12] W. Morong, F. Liu, P. Becker, K. S. Collins, L. Feng, A. Kyprianidis, G. Pagano, T. You, A. V. Gorshkov, and C. R. Monroe, Publisher correction: Observation of Stark many-body localization without disorder, Nature (London) **601**, e13 (2022).

[13] H. Lang, P. Hauke, J. Knolle, F. Grusdt, and J. C. Halimeh, Disorder-free localization with Stark gauge protection, Phys. Rev. B **106**, 174305 (2022).

[14] Y.-Y. Wang, Z.-H. Sun, and H. Fan, Stark many-body localization transitions in superconducting circuits, Phys. Rev. B **104**, 205122 (2021).

[15] C. Gao, Z. Tang, F. Zhu, Y. Zhang, H. Pu, and L. Chen, Nonthermal dynamics in a spin-$\frac{1}{2}$ lattice Schwinger model, Phys. Rev. B **107**, 104302 (2023).

[16] G.-Y. Zhu and M. Heyl, Subdiffusive dynamics and critical quantum correlations in a disorder-free localized Kitaev honeycomb model out of equilibrium, Phys. Rev. Res. **3**, L032069 (2021).

[17] L. Wadleigh, N. G. Kowalski, and B. Demarco, Interacting Stark localization dynamics in a three-dimensional lattice Bose gas, Phys. Rev. A **107**, 043325 (2023).

[18] N. Zhang, Y. Ke, L. Lin, L. Zhang, and C. Lee, Stable interaction-induced Anderson-like localization embedded in standing waves, New J. Phys. **25**, 043021 (2023).

[19] A. Peres, Stability of quantum motion in chaotic and regular systems, Phys. Rev. A **30**, 1610 (1984).

[20] A. Goussev, R. Jalabert, H. M. Pastawski, and D. A. Wisniacki, Loschmidt echo, Scholarpedia **7**, 11687 (2012).

[21] D. A. Abanin, E. Altman, I. Bloch, and M. Serbyn, *Colloquium*: Many-body localization, thermalization, and entanglement, Rev. Mod. Phys. **91**, 021001 (2019).

[22] A. Kitaev, A simple model of quantum holography, KITP program: Entanglement in strongly-correlated quantum matter, available at https://online.kitp.ucsb.edu/online/entangled15/.

[23] S. Sachdev and J. Ye, Gapless spin-fluid ground state in a random quantum Heisenberg magnet, Phys. Rev. Lett. **70**, 3339 (1993).

[24] J. Maldacena, S. H. Shenker, and D. Stanford, A bound on chaos, J. High Energy Phys. 08 (2016) 106.

[25] V. Rosenhaus, An introduction to the SYK model, J. Phys. A: Math. Theor. **52**, 323001 (2019).

[26] J. Kempe, Quantum random walks: An introductory overview, Contemp. Phys. **44**, 307 (2003).

[27] S. E. Venegas-Andraca, Quantum walks: A comprehensive review, Quantum Inf. Process. **11**, 1015 (2012).

[28] D. Reitzner, D. Nagaj, and V. R. Buzek, Quantum walks, Acta Phys. Slovaca **61**, 603 (2011).

[29] A. M. Childs, E. Farhi, and S. Gutmann, An example of the difference between quantum and classical random walks, Quantum Inf. Process. **1**, 35 (2001).

[30] A. Ambainis, E. Bach, A. Nayak, A. Vishwanath, and J. Watrous, in *Proceedings of the 33rd Annual ACM Symposium on the Theory of Computing, Hersonissos, 2001* (ACM, New York, 2001), pp. 37–49.

[31] Y. Aharonov, L. Davidovich, and N. Zagury, Quantum random walks, Phys. Rev. A **48**, 1687 (1993).

[32] M. Santha, in *Theory and Applications of Models of Computation*, edited by M. Agrawal, D. Du, Z. Duan, and A. Li, Lecture Notes in Computer Science, Vol. 4978 (Springer, Berlin, 2008).

[33] N. Shenvi, J. Kempe, and K. B. Whaley, Quantum random-walk search algorithm, Phys. Rev. A **67**, 052307 (2003).

[34] R. Portugal, *Quantum Walks and Search Algorithms* (Springer, Berlin, 2013).

[35] K. Bepari, S. Malik, M. Spannowsky, and S. Williams, Quantum walk approach to simulating parton showers, Phys. Rev. D **106**, 056002 (2022).

[36] B. P. Nachman, D. Provasoli, W. A. de Jong, and C. W. Bauer, Quantum algorithm for high energy physics simulations, Phys. Rev. Lett. **126**, 062001 (2021).

[37] R. D. Somma, S. Boixo, H. Barnum, and E. Knill, Quantum simulations of classical annealing processes, Phys. Rev. Lett. **101**, 130504 (2008).

[38] F. W. Strauch, Relativistic quantum walks, Phys. Rev. A **73**, 054302 (2006).

[39] A. M. Childs, D. Gosset, and Z. Webb, Universal computation by multiparticle quantum walk, Science **339**, 791 (2013).

[40] M. S. Underwood and D. L. Feder, Universal quantum computation by discontinuous quantum walk, Phys. Rev. A **82**, 042304 (2010).

[41] R. Asaka, K. Sakai, and R. Yahagi, Two-level quantum walkers on directed graphs. I. Universal quantum computing, Phys. Rev. A **107**, 022415 (2023).

[42] A. M. Childs, Universal computation by quantum walk, Phys. Rev. Lett. **102**, 180501 (2009).

[43] L. Sansoni, F. Sciarrino, G. Vallone, P. Mataloni, A. Crespi, R. Ramponi, and R. Osellame, Two-particle bosonic-fermionic quantum walk via integrated photonics, Phys. Rev. Lett. **108**, 010502 (2012)

[44] X. Qin, Y. Ke, X.-W. Guan, Z. Li, N. Andrei, and C. Lee, Statistics-dependent quantum co-walking of two particles in one-dimensional lattices with nearest-neighbor interactions, Phys. Rev. A **90**, 062301 (2014).

[45] M. K. Giri, S. Mondal, B. P. Das, and T. Mishra, Two component quantum walk in one-dimensional lattice with hopping imbalance, Sci. Rep. **11**, 22056 (2021).

[46] A. A. Melnikov and L. Fedichkin, Quantum walks of interacting fermions on a cycle graph, Sci. Rep. **6**, 34226 (2016).

[47] A. A. Melnikov, A. P. Alodjants, and L. Fedichkin, in *Proceedings of the International Conference on Micro- and*

Nano-Electronics, Zvenigorod, 2018, edited by V. F. Lukichev and K. V. Rudenko, SPIE Proc. Vol. 11022 (SPIE, Bellingham, 2018).

[48] Y. Lahini, M. Verbin, S. D. Huber, Y. Bromberg, R. Pugatch, and Y. R. Silberberg, Quantum walk of two interacting bosons, Phys. Rev. A **86**, 011603(R) (2012).

[49] D. Wiater, T. Sowi'nski, and J. J. Zakrzewski, Two bosonic quantum walkers in one-dimensional optical lattices, Phys. Rev. A **96**, 043629 (2017).

[50] H. Krovi, Symmetry in quantum walks, Ph.D. thesis, University of Southern California, 2007.

[51] J. Janmark, D. A. Meyer, and T. G. Wong, Global symmetry is unnecessary for fast quantum search, Phys. Rev. Lett. **112**, 210502 (2014).

[52] C. M. Chandrashekar, R. Srikanth, and S. Banerjee, Symmetries and noise in quantum walk, Phys. Rev. A **76**, 022316 (2007).

[53] C. Cedzich, T. Geib, F. A. Grünbaum, C. Stahl, L. Velázquez, A. H. Werner, and R. F. Werner, The topological classification of one-dimensional symmetric quantum walks, Ann. Henri Poincaré **19**, 325 (2018).

[54] C. Cedzich, T. Geib, F. A. Grünbaum, L. Vel'azquez, A. H. Werner, and R. F. Werner, Quantum walks: Schur functions meet symmetry protected topological phases, Commun. Math. Phys. **389**, 31 (2012).

[55] C. Cedzich, J. Fillman, T. Geib, and A. H. Werner, Singular continuous Cantor spectrum for magnetic quantum walks, Lett. Math. Phys. **110**, 1141 (2020).

[56] C. Cedzich, T. Geib, C. Stahl, L. Velázquez, A. H. Werner, and R. F. Werner, Complete homotopy invariants for translation invariant symmetric quantum walks on a chain, Quantum **2**, 95 (2018).

[57] B. Danacı, I. Yalçinkaya, B. Çakmak, G. Karpat, S. P. Kelly, and A. L. Subaşı, Disorder-free localization in quantum walks, Phys. Rev. A **103**, 022416 (2021).

[58] A. Mandal, R. S. Sarkar, and B. Adhikari, Localization of two dimensional quantum walks defined by generalized grover coins, J. Phys. A: Math. Theor. **56**, 025303 (2023).

[59] S. Singh and C. M. Chandrashekar, Interference and correlated coherence in disordered and localized quantum walk, arXiv:1711.06217.

[60] A. Joye, Dynamical localization for d-dimensional random quantum walks, Quantum Inf. Process. **11**, 1251 (2012).

[61] C. Cedzich and A. H. Werner, Anderson localization for electric quantum walks and skew-shift CMV matrices, Commun. Math. Phys. **387**, 1257 (2021).

[62] H. Gerhardt and J. Watrous, in *Approximation, Randomization, and Combinatorial Optimization. Algorithms and Techniques*, edited by S. Arora, K. Jansen, J. D. P. Rolim, and A. Sahai, Lecture Notes in Computer Science Vol. 2764 (Springer, Berlin, 2003), pp. 290–301.

[63] E. Brézin and S. Hikami, Spectral form factor in a random matrix theory, Phys. Rev. E **55**, 4067 (1997).

[64] J. S. Cotler, G. Gur-Ari, M. Hanada, J. Polchinski, P. Saad, S. H. Shenker, D. Stanford, A. Streicher, and M. Tezuka, Black holes and random matrices, J. High Energy Phys. 05 (2017) 118.

[65] G. Cipolloni, L. Erdős, and D. Schröder, On the spectral form factor for random matrices, Commun. Math. Phys. **401**, 1665 (2023).

[66] C. Arenz, G. Gualdi, and D. Burgarth, Control of open quantum systems: Case study of the central spin model, New J. Phys. **16**, 065023 (2014).

[67] R. I. Nepomechie and X.-W. Guan, The spin-s homogeneous central spin model: Exact spectrum and dynamics, J. Stat. Mech. 103104 (2018).

[68] T. Villazon, P. W. Claeys, M. Pandey, A. Polkovnikov, and A. Chandran, Persistent dark states in anisotropic central spin models, Sci. Rep. **10**, 16080 (2020).

[69] C. D. Godsil, Sedentary quantum walks, Linear Algebra Appl. **614**, 356 (2021).

[70] W. Carlson, A. For, E. Harris, J. Rosen, C. Tamon, and K. Wrobel, Universal mixing of quantum walk on graphs, Quantum Inf. Comput. **7**, 738 (2006).

[71] X. Xu, Exact analytical results for quantum walks on star graphs, J. Phys. A: Math. Theor. **42**, 115205 (2009).

[72] M. Frigerio and M. G. Paris, Swift chiral quantum walks, Linear Algebra Appl. **673**, 28 (2023).

[73] C. D. Godsil, When can perfect state transfer occur, arXiv:1011.0231.

[74] Y. Ide, Local subgraph structure can cause localization in continuous-time quantum walk, Math. J. **60**, 113 (2014).

[75] C. D. Godsil and G. F. Royle, *Algebraic Graph Theory*, Graduate Texts in Mathematics Vol. 207 (Springer, Berlin, 2001).

[76] A. E. Brouwer and W. H. Haemers, *Spectra of Graphs* (Springer, New York, 2011).

[77] D. I. Tsomokos, S. Ashhab, and F. Nori, Fully connected network of superconducting qubits in a cavity, New J. Phys. **10**, 113020 (2008).

[78] K. Xu, Z.-H. Sun, W. Liu, Y.-R. Zhang, H. Li, H. Dong, W. Ren, P. Zhang, F. Nori, D. Zheng, H. Fan, and H. Wang, Probing the dynamical phase transition with a superconducting quantum simulator, Sci. Adv. **6**, eaba4935 (2020).

[79] C. Song, K. Xu, H. Li, Y.-R. Zhang, X. Zhang, W. Liu, Q. Guo, Z. Wang, W. Ren, J. Hao, H. Feng, H. Fan, D. Zheng, D.-W. Wang, H. Wang, and S.-Y. Zhu, Generation of multicomponent atomic Schrödinger cat states of up to 20 qubits, Science **365**, 574 (2019).

[80] S. Hazra, A. Bhattacharjee, M. Chand, K. V. Salunkhe, S. Gopalakrishnan, M. P. Patankar, and R. Vijay, Long-range connectivity in a superconducting quantum processor using a ring resonator, Phys. Rev. Appl. **16**, 024018 (2021).

[81] B. P. Lanyon, C. Hempel, D. Nigg, M. Müller, R. Gerritsma, F. Zähringer, P. Schindler, J. T. Barreiro, M. Rambach, G. Kirchmair, M. Hennrich, P. Zoller, R. Blatt, and C. F. Roos, Universal digital quantum simulation with trapped ions, Science **334**, 57 (2011).

[82] K. Wright, K. M. Beck, S. Debnath, J. M. Amini, Y. S. Nam, N. Grzesiak, J.-S. Chen, N. C. Pisenti, M. Chmielewski, C. Collins, K. M. Hudek, J. Mizrahi, J. D. Wong-Campos, S. Allen, J. Apisdorf, P. Solomon, M. Williams, A. M. Ducore, A. Blinov, S. M. Kreikemeier *et al.*, Benchmarking an 11-qubit quantum computer, Nat. Commun. **10**, 5464 (2019).

[83] M. A. Cazalilla and A. M. Rey, Ultracold Fermi gases with emergent SU(N) symmetry, Rep. Prog. Phys. **77**, 124401 (2014).

[84] K. Hashimoto, K. Murata, and R. Yoshii, Out-of-time-order correlators in quantum mechanics, J. High Energy Phys. 10 (2017) 138.

[85] A. P. Balachandran, T. R. Govindarajan, A. R. de Queiroz, and A. F. Reyes-Lega, Entanglement and particle identity: A unifying approach, Phys. Rev. Lett. **110**, 080503 (2013).

[86] A. P. Balachandran, T. R. Govindarajan, A. R. de Queiroz, and A. F. Reyes-Lega, Algebraic approach to entanglement and entropy, Phys. Rev. A **88**, 022301 (2013).

[87] A. F. Reyes-Lega, Entanglement entropy in quantum mechanics: An algebraic approach, *Particles, Fields and Topology Celebrating AP Balachandran* (World Scientific, 2023), pp. 191–199.

[88] A. P. Balachandran, A. Queiroz, and S. Vaidya, Entropy of quantum states: Ambiguities, Eur. Phys. J. Plus **128**, 112 (2013).

[89] A. P. Balachandran, A. Queiroz, and S. Vaidya, Quantum entropic ambiguities: Ethylene, Phys. Rev. D **88**, 025001 (2013).

[90] F. Benatti, R. Floreanini, F. Franchini, and U. Marzolino, Entanglement in indistinguishable particle systems, Phys. Rep. **878**, 1 (2020).